Elsevier Editorial System(tm) for Cell
Manuscript Draft

Manuscript Number: CELL-D-11-01251R1

Title: Key ceRNA role for the long non-coding RNA linc-MD1 in the control of muscle differentiation

Article Type: Research Article

Keywords: long non-coding RNA; lincRNA; ceRNA; miRNA; miR-133; miR-135; muscle differentiation; MEF2C; MAML1; DMD

Corresponding Author: Dr. Irene Bozzoni,

Corresponding Author's Institution:

First Author: Marcella Cesana

Order of Authors: Marcella Cesana; Davide Cacchiarelli; Ivano Legnini; Tiziana Santini; Olga Sthandier; Mauro Chinappi; Anna Tramontano; Irene Bozzoni

Abstract: The inventory of biological processes in which non-coding RNAs are involved is continuously enriched. Recently, a new regulatory circuitry has been identified in which coding and non-coding RNAs can cross-talk to each other by competing for miRNA binding via their miRNA recognition motifs. Such competing endogenous RNAs (ceRNAs) act as "decoys" impacting on the distribution of miRNA molecules on their targets and thereby imposing an additional level of post-transcriptional regulation. Here we show that long non-coding RNAs also play a relevant role in the complex network of regulatory interactions governing muscle differentiation. We identified a conserved muscle-specific long non-coding cytoplasmic RNA, linc-MD1, which acts as a ceRNA. Modulation of linc-MD1 expression and mutant analyses indicated that it controls muscle differentiation both in mouse and human myoblasts. Among the targets of the "decoyed" miRNAs, we identified MAML1 and MEF2C, two factors playing a relevant role in activation of muscle-specific gene expression.

Suggested Reviewers:

Opposed Reviewers:

***Cover Letter (required for ALL submissions)**

Rome, 9 September 2011

Ref. #: CELL-D-11-01251

Dear Editor,
please find in attachment the revised copy of the manuscript " Key ceRNA role for the long non-coding RNA linc-MD1 in the control of muscle differentiation" by Cesana et al. that we revised according to the reviewers' comments. The point to point response is attached in file "response to reviewers"

Best regards,
Irene Bozzoni

***Abstract (required for ALL submissions)**

The inventory of biological processes in which non-coding RNAs are involved is continuously enriched. Recently, a new regulatory circuitry has been identified in which coding and non-coding RNAs can cross-talk to each other by competing for miRNA binding via their miRNA recognition motifs. Such competing endogenous RNAs (ceRNAs) act as “decoys” impacting on the distribution of miRNA molecules on their targets and thereby imposing an additional level of post-transcriptional regulation. Here we show that long non-coding RNAs also play a relevant role in the complex network of regulatory interactions governing muscle differentiation. We identified a conserved muscle-specific long non-coding cytoplasmic RNA, linc-MD1, which acts as a ceRNA. Modulation of linc-MD1 expression and mutant analyses indicated that it controls muscle differentiation both in mouse and human myoblasts. Among the targets of the "decoyed" miRNAs, we identified MAML1 and MEF2C, two factors playing a relevant role in activation of muscle-specific gene expression.

***Response to Reviewers (required for REVISED submissions)**

CELL-D-11-01251

Dear Editor,
please find in attachment the revised copy of the manuscript " Key ceRNA role for the long non-coding RNA linc-MD1 in the control of muscle differentiation" by Cesana et al. that we revised according to the reviewers' comments

Here below the point to point reply to each criticism

Reviewer #1

1) The most valuable piece of evidence would be the direct detection of Ago binding to linc-MD1 in a miR133/135-dependent manner. By now this should be technically feasible for the authors to at least attempt.

The only Ago antibodies that we were able to get in short time were the human ones from Gunter Meister's lab. Unfortunately, it was impossible to perform the experiment with human cells since for immunoprecipitation of Ago-containing complexes (in order to analyze target mRNA) approximately 20-30 x 10^6 cells are needed. This amount is far beyond what we can get with the human myoblasts (primary cells) utilized in this work. Therefore, we performed the experiment with C2 mouse myoblasts. The results were negative even for the detection of the miRNA components (also in overexpression conditions), indicating that the human Ago antibodies are not suitable for IP in mouse.
At this point we would need either to purchase mouse-specific Ago antibodies or to get an Ago-FLAG construct in order to perform FLAG IP. It will take quite sometime to get the reagents and to set up the right IP conditions; therefore, this wouldn't allows us to comply with the requested reviewing time. However, this is certainly a type of experiment that we will be doing in future analysis.

2) If the primary role of linc-MD1 is to directly sequester miR133/135, then the introduction of anti-miRNA LNAs should not only phenocopy linc-MD1 overexpression (Figure S6) but should do so in a dose-dependent manner, and should also overcome the effects of linc-MD1 knockdown. Overall the LNAs are valuable tools that are underused in this work.

We have performed a new experiment where we have tested the effect of LNA (against miR-133 and miR-135) treatment in conditions of linc-MD1 depletion (RNAi). With respect to the linc-MD1 knock down (RNAi) alone where the levels of the MAML1 and MEF2C decrease, the additional depletion of miRNAs (RNAi+LNA) resumes protein synthesis producing a perfect phenocopy of linc-overexpression. We have produced a new Figure 6B comparing all these different treatments: i) LNA against miR-135 and miR-133, ii) RNAi against linc-MD1, iii) a combination of LNA+RNAi and iV) linc-MD1 overexpression. The overal data are very consistent with the model of a specific cross-talk between linc-MD1 and MAML1 and MEF2C mRNAs through competition for miR-133 and miR-135 binding.

Moreover, we have also performed experiments where LNA oligos were tested with luc constructs containing the 3'UTR of MAML1 and MEF2C. The data (included in Figure S5B) further support the finding that these sequences are target of miR-133 and miR-135, respectively.

3) In Figure 5C the authors show that the maml1-mut and mef2c-mut reporters (from which

the proposed miRNA binding sites are deleted) fail to respond to mir133/135 overexpression, and then in Figure 5D show that maml1-WT and mef2c-WT reporters are upregulated in response to linc-MD1 overexpression. The critical last step of this analysis is to show that the maml1-mut and mef2c-mut reporters are not upregulated when linc-MD1 is overexpressed. It is not clear why the authors did not do this.

We had such controls. We have added them into the new Figure 5D.

Two more minor comments:

1) It can be dangerous to define a transcript as non-coding given the increasing number of reports of small peptides generated from ORFs that are below some arbitrary cut-off. The status of linc-MD1 as an ncRNA seems likely but at the very least the authors should state that the ORF that starts at the first AUG downstream of the defined TSS is only X codons long, whatever X happens to be. They could also choose to comment on whether that AUG does or does not deviate from the Kozak consensus. The readers would then be better able to judge for themselves whether linc-MD1 might have protein-coding potential.

We have performed such analysis which is now included in Figure S1B.
The mature linc-MD1 transcript does contain four open reading frames (defined as any sequence starting with AUG and containing at least 10 non terminator codons) ranging in size from 11 to 91 triplets. However, none of the AUG shows a Kozak consensus, nor are the sequences more or less conserved than the surrounding regions. Although it cannot be formally excluded that some parts of the linc-MD1 are translated, it is quite unlikely that this is the case. We have introduced the data as Figure S1B and referred to this analysis in the text.

2) It seems a bit premature to describe linc-MD1 as "restricted to skeletal muscles" (third paragraph of Results) when the only other tissues examined are liver and heart. The authors need to either examine a greater variety of tissues or else limit the strength of their claim.

We have performed linc-MD1 expression analysis on a collection of different tissues (testis, seminal vesicles, liver, heart, brain, spleen, kidney, lung, intestine and skeletal muscle). The expression remains at background levels in all tissues but skeletal muscles. We have included these data in Figure S1C and have rephrased the sentence in the text.

Reviewer #2:
1. In figure 6A, the expression of miR-133 and miR-135 are graphed as "copy number", according to the figure legend. However, these values seem minute. Is that copy number per a particular number of cells or mass of RNA? If the denominator is not meaningful, it may be more appropriate to graph the relative expression, as has been done in other figures throughout the manuscript.

In Figure 6A the copy number was referred to ng of RNA. We have changed this into relative expression as suggested.

2. Figure 6A shows that miR-135 increases ~10 fold during the course of mouse C2

myoblast differentiation. In contrast, Figure 7A shows that miR-135 expression decreases by about 80% during human myoblast differentiation. However, the authors make the argument that linc-MD1 is required to sequester miR-135 allowing Mef2c translation and myoblast differentiation. Is this inconsistent with the observed miR-135 decrease during human myoblast differentiation? Is there an explanation for the species/cell type difference in miR-135 dynamics? Please acknowledge.

It is true that during human myoblast differentiation we observed a decrease of miR-135 at difference with mouse C2 cells. However, it is difficult to compare the two types of cells: while C2 myoblasts represent a homogeneous line with features of precursor cells (they still express the stemness factor Pax7), the human primary myoblasts utilized derive from a tissue biopsis including more heterogeneous cell types. Moreover, the latter display a different timing of differentiation: they differentiate and fuse much more efficiently than C2 myoblasts and they do not express Pax7.

Minor Issues:

1. On page 8, next to last paragraph, 3rd line, "myoblast" is misspelled.
OK

2. The model diagram in Figure 7c is weak in that it does not fully depict the proposed sequestration of miRNAs away from their target mRNAs by linc-MD1. Perhaps a two-paneled diagram illustrating the activity of miR-135 and miR-133 during growth conditions and then in differentiation conditions would better illustrate how linc-MD1 regulates the activity of

We have modified the figure.

If you and the referees agree we would like to add the following information which strengthens the concept of linc-MD1 being a sponge for miRNAs: in line with a "decoy" mechanism, the predicted ΔG of binding (Enright et al,2003) of the miRNAs with linc-MD1 was found to be lower than that with the respective targets. This info has been added in the new Figure S6.

We hope that with these modifications the paper will be now suitable for publication and we thank you again for the interest in our work.
Best regards,
Irene Bozzoni

Key ceRNA role for the long non-coding RNA linc-MD1 in the control of muscle differentiation

Cesana Marcella[1§], Cacchiarelli Davide[1§], Legnini Ivano[1], Santini Tiziana[1], Sthandier Olga[1], Chinappi Mauro[2], Tramontano Anna[2,3,4] and Bozzoni Irene[1,3,4,5,*]

[1]Dept. of Biology and Biotechnology "Charles Darwin"
[2]Dept. of Physics,
[3]Institut Pasteur Fondazione Cenci-Bolognetti,
[4]Center for Life Nano Science @Sapienza, Istituto Italiano di Tecnologia,
Sapienza University of Rome, P.le A. Moro 5, 00185 Rome
[5]IBPM of CNR

[§]These authors contributed equally to the work
* Corresponding author: irene.bozzoni@uniroma1.it

Keywords: long non-coding RNA; lincRNA; ceRNA; miRNA; miR-133; miR-135; muscle differentiation; MEF2C; MAML1; DMD

Abstract

The inventory of biological processes in which non-coding RNAs are involved is continuously enriched. Recently, a new regulatory circuitry has been identified in which coding and non-coding RNAs can cross-talk to each other by competing for miRNA binding via their miRNA recognition motifs. Such competing endogenous RNAs (ceRNAs) act as “decoys” impacting on the distribution of miRNA molecules on their targets and thereby imposing an additional level of post-transcriptional regulation. Here we show that long non-coding RNAs also play a relevant role in the complex network of regulatory interactions governing muscle differentiation. We identified a conserved muscle-specific long non-coding cytoplasmic RNA, linc-MD1, which acts as a ceRNA. Modulation of linc-MD1 expression and mutant analyses indicated that it controls muscle differentiation both in mouse and human myoblasts. Among the targets of the "decoyed" miRNAs, we identified MAML1 and MEF2C, two factors playing a relevant role in activation of muscle-specific gene expression.

Introduction

One of the greatest surprises of high throughput transcriptome analysis of the last years has been the discovery that the mammalian genome is pervasively transcribed into many different complex families of RNA. In addition to a large number of alternative transcriptional start sites, termination and splicing patterns, a complex collection of new antisense, intronic and intergenic transcripts was found. Moreover, almost half of the polyadenylated species resulted to be non-protein-coding RNAs. Although many studies have helped unveiling the function of many small non-coding RNAs, very little is known about the long non-coding (lncRNA) counterpart of the transcriptome. In spite of their very low levels of expression in specific body compartments and thanks to the availability of sensitive detection techniques, specific patterns of lncRNA expression in specific cell types, tissues and developmental conditions (Amaral and Mattick 2008; Qureshi et al., 2010) have been defined.

So far, a large range of functions has been attributed to lncRNAs (Mattick, 2011; Nagano and Fraser, 2011), such as modulation of apoptosis and invasion (Khaitan et al., 2011), reprogramming of induced pluripotent stem cells (Loewer et al., 2010), marker of cell fate (Ginger et al., 2006) and parental imprinting (Sleutels et al., 2002), indicating that they may represent a major regulatory component of the eukaryotic genome.

A specific mode of action in mediating epigenetic changes through recruitment of the Polycomb Repressive Complex (PRC) was described for the Xist and HOTAIR transcripts (Chaumeil et al., 2006; Rinn et al., 2007). lncRNAs were also found to act in the nucleus as antisense transcripts or as decoy for splicing factors leading to splicing malfunctioning (Beltran et al., 2008; Tripathi et al, 2010). In the cytoplasm, lncRNAs were described to transactivate STAU1-mediated mRNA decay by duplexing with 3' UTRs via Alu elements (Gong and Maquat, 2011) or, in the case of pseudogenes, to compete for miRNA binding, thereby modulating the derepression of miRNA targets (Poliseno et al., 2010; Salmena et al., 2011).

These findings have obviously prompted studies directed towards the identification of the circuitries that are regulated by these molecules.

Muscle differentiation is a powerful system for these investigations both because it can be recapitulated *in vitro* and because the networks of transcription factors coordinating the expression of genes involved in muscle growth, morphogenesis and differentiation are well

known and evolutionarily conserved (Buckingham and Vincent, 2009). Moreover, recent studies have shown that these myogenic transcription factors not only control protein-coding genes, but also regulate the expression of specific miRNAs (Zhao et al., 2005; Rao et al., 2006). These miRNAs act at different levels in the modulation of muscle differentiation and homeostasis and their expression was found to be altered in several muscular disorders such as myocardial infarction, Duchenne Muscular Dystrophy and other myopathies (Eisenberg et al., 2007; Cacchiarelli et al., 2010).

Among microRNAs specifically expressed in muscle tissue, the most widely studied are members of the miR-1/206 and miR-133a/133b families, which originate from three separate chromosomes (Chen et al., 2006). miR-206 differs from other members of its family because it is exclusive of skeletal muscles (McCharty, 2008). Moreover, at variance with other myomiRs mainly expressed in mature muscle fibers, miR-206 expression is enriched in differentiating satellite cells, where it represses the stemness factor Pax7, a crucial player in the regeneration process, as we recently demostrated (Cacchiarelli et al., 2010).

In this study, through a detailed analysis of the genomic region of miR-206/133b, we discovered the existence of a muscle specific lincRNA and defined its expression profile and function. We demonstrated that this lincRNA is involved in the timing of muscle differentiation and acts as a natural decoy for miRNAs, playing a crucial role in the control of factors involved in the myogenic program.

RESULTS

linc-MD1 is expressed during myoblasts differentiation

miRNA coding regions display different genomic organizations: while 50% are encoded in introns or exons of protein coding genes, the other half map in ncRNA host genes or, when no host transcript can be identified, in intergenic regions (Figure 1A). According to this classification, muscle specific pre-miR-206 and pre-miR-133b were annotated as overlapping with a noncoding RNA (Williams et al. 2009). With the aim of better understanding the transcriptional regulation of these two microRNAs, we carried out a detailed analysis in order to identify their transcriptional start sites (TSS) and promoter elements. 5’ race analysis, performed in differentiating myoblasts with reverse primers surrounding the pre-miR-206 sequence, demonstrated the existence of a proximal TSS

mapping about 600 bp upstream of the pre-miR-206 sequence (proximal, Figure 1B). This region contains E-box sequences (CANNTG) previously shown to be functional for MyoD association (Rao et al.2006) and mir-206 expression (Williams et al. 2009). The same analysis was also performed with reverse primers surrounding pre-miR-133b. A strong TSS, mapping approximately 13 Kb upstream of pre-miR-133b sequence, was identified (distal, Figure 1B). Analysis of the genomic region revealed the existence of a transcript composed of three exons and two introns; with respect to this structure, pre-miR-206 maps in the second intron, while pre-miR-133b in the third exon (Figure 1B and Figure S1). Even if short reading frames can be detected in the mature transcript, none of their AUGs shows the Kozak consensus nor are their sequences more or less conserved than the surrounding regions (Figure S1B), making it very unlikely for them to be coding. Therefore, the identified transcript was classified as a *bona-fide* long intergenic non-coding (linc) RNA, hereafter termed linc-MD1. Phylogenetic analysis of linc-MD1 revealed high conservation in exon 1 and 2, while homology is limited to the pre-mir-133b sequence in exon 3 (Figure 1B). All splice junctions are conserved as well. *In silico* analysis highlighted the presence of conserved E-boxes both in the DIST and PROX regions (Figure 1B) as well as in the regions surrounding the second exon where minor alternative TSSs were mapped (not shown).

RT-PCR analysis (Figure 1C) indicates that linc-MD1 is localized in the cytoplasm and is polyadenylated. Moreover, while absent in growth conditions (GM), linc-MD1 is activated upon shift to differentiation (DM) of mouse myoblasts, satellite cells and MyoD-transdifferentiated fibroblasts. The expression level of linc-MD1 parallels that of miR-133b upon induction of differentiation, while it is uncoupled from the miR-206 expression, which is already present in proliferating C2 myoblasts. The two bands detected by RT-PCR reveal the presence of a 70 nucleotide splice variant in exon 2. Northern blot analysis of poly-A+ RNA from differentiating myoblasts indicates that linc-MD1 is indeed the major pA+ product originating from this region, even though the two alternative splice forms are not distinguishable on this gel (Figure 1D). *In situ* analysis confirms that linc-MD1 is not expressed in proliferating conditions while it is induced upon myoblast differentiation (Figure 1F).

RT-PCR analysis of linc-MD1 in mouse tissues (Figure 1E) indicates that it is highly expressed in skeletal muscles of dystrophic *mdx* animals (TIB and SOL), paralleling miR-206 and miR-133b synthesis. Notably, in wild-type animals linc-MD1 is expressed at low levels only in the soleus, while it is absent in tibialis and other skeletal muscles (not

shown). No linc-MD1 expression is observed in non muscle tissues (LIV and Figure S1C) nor in heart (HEA), thus indicating that also linc-MD1, similarly to miR-206, is restricted to skeletal muscles. *In situ* analysis (Figure 1G) on WT and *mdx* muscles indicates that linc-MD1 expression occurs exclusively in newly regenerating fibers (characterized by centronucleated fibers), abundant in dystrophic conditions, similarly to what previously shown for miR-206 (Cacchiarelli et al., 2010, Yuasa et al. 2008). No expression is instead detected in mature terminally differentiated fibers, as shown in wild-type animals devoid of regenerating fibers. The low level of linc-MD1 found in the soleus would therefore suggest that some degree of regeneration occurs in this district known to have a high content of satellite cells (Chargè and Rudkini, 2004).
These data indicate that linc-MD1 is muscle-specific and is activated upon myoblast differentiation.

Identification of regulatory elements directing linc-MD1 and miR-206/133b expression

Promoter fusion experiments with the Distal (DIST) and Proximal (PROX) regions were performed in order to test their role in transcription. 810 and 310 nucleotides of DIST and PROX regions, respectively, were cloned upstream of either the murine pre-miR-223 (Ballarino et al., 2009) sequence (D-miR-223 and P-miR-223) or the firefly luciferase coding region (D-FLuc and P-FLuc). Their promoter activity was tested in mouse C2 myoblasts in proliferation (GM, white bars) versus differentiation (DM, black bars) conditions. Figure 2A shows that the PROX element is already active in GM, in agreement with basal miR-206 expression (see Figure 1C). Upon induction of differentiation, the proximal region is able to further induce the expression of both reporter genes (miR-223 and FLuc). On the contrary, the DIST element is inactive in GM while, upon shift to differentiation, is able to activate transcription. Notably, when the PROX and DIST elements are present on the same construct they act synergistically, providing the strongest activation (D-Fluc-P and P-Fluc-D).
As indicated in Figure 1B, both regions contain E-box elements and indeed both of them are able to bind MyoD *in vivo,* as demonstrated by chromatin immunoprecipitation analysis (Figure 2B). MyoD binding to DIST in GM conditions is in line with the notion that MyoD binds promoters prior to transcriptional activation, which occurs upon its acetylation.

Nine regions spanning the entire locus (A-I, Figure 2C) were tested for the major markers of chromatin modifications in both GM and DM conditions. Consistently with the promoter fusion analysis, RNA polymerase II (RNAPII) enrichment is observed on the PROX promoter already in GM. Interestingly, in these conditions, no polymerase is found on miR-133b indicating that the PROX promoter does not direct transcriptional read-through into this region. These data are in agreement with the observation that miR-133b expression is uncoupled from that of miR-206. Upon induction of differentiation, RNAPII immunoprecipitates on the DIST promoter and on the entire region: RNAPII enrichment decreases gradually along the cluster and increases at the 3' end in a fashion similar to that of many transcriptional units (Moore and Proudfoot, 2009). Histone-H3-lysine-9 acetylation (H3K9ac) and Histone-H3-lysine-27 tri-methylation (H3K27me3) patterns are in agreement with the differential transcriptional activity of the two promoters: low H3K27me3 and high H3K9ac immunoprecipitation levels are found on the PROX element already in GM and are maintained in DM (highlighted in grey). Conversely, DIST displays low H3K9ac and high H3K27me3 signature in GM, while the pattern is reverted upon differentiation, in line with transcriptional activation (highlighted in grey). Notably, the H3K4me3 marker, enriched around TSS of active RNAPII promoters (Okitsu et al., 2010), confirmed the presence of TSS on the distal region in DM conditions (Figure 2C, lower panel). Interestingly, 3meH3K4 was detected also in region C where minor TSS were mapped (not shown), suggesting the presence of additional transcripts in this region.
Altogether, our data indicated that the PROX promoter is responsible for miR-206 expression in growth conditions, while upon differentiation both PROX and DIST cooperate to drive transcription of the locus.

Distal and Proximal promoters are involved in long distance interactions

Since promoter fusion assays demonstrated cooperation between the DIST and PROX elements, we investigated whether these two regions could physically interact *in vivo*. Gene loops have been shown to be transcriptionally dependent, as they are absent in non-transcribing conditions (West and Fraser, 2005). Chromosome Conformation Capture (3C) analysis (Tan-Wong et al., 2008) was utilized to determine relative cross-linking frequencies among the regions of interest. The conformation of the miR-206/133b genomic locus was initially tested in myoblasts, both in GM and DM conditions, as well as in fibroblasts where the two miRNAs are not expressed. A common reverse primer

(indicated by X in Figure 3A) mapping in the PROX region was used in combination with a set of primers along the genomic locus and interactions were analyzed by qPCR (Figure 3A; note that A-I sites correspond to the same regions analyzed in ChIP experiments). A specific interaction between PROX and DIST region (X-B) is observed upon induction of differentiation. A less prominent but reproducible interaction is also detected between X and the I, which identifies the polyadenylation region (pA). No specific long-range interactions were detected in fibroblasts where the locus is silent.
An interaction, clearly distinguishable from the background, is also found with the A region. This can be due to its proximity to the DIST element or it can point to the existence of an additional enhancer region.

3C analysis was also performed in different types of mouse tissues from WT and *mdx* animals. Figure 3B shows that the interaction between the PROX and DIST regions only occurs in skeletal muscles and it is characteristic of muscles with high regeneration rate, such as the soleus (Chargé and Rudnicki, 2004). Notably, PROX-DIST interaction is particularly enhanced in *mdx* muscles, known to undergo intense regeneration (*mdx* SOL). The same specificity was also detected for the PROX-pA interaction (Figure 3B, X-I); on the contrary, no relevant interaction was detected between PROX and a negative control region (X-Y).
From these data we concluded that the long-distance interaction between the DIST and PROX is functional to both linc-MD1 and miRNAs expression. Figure 3C schematically shows the looping structure correlated with the activation state of the locus.

Modulation of linc-MD1 expression affects myogenic differentiation

Figure 4A shows the expression profiles of myogenic protein markers (Myogenin - MYOG and Myosin Heavy Chain - MHC), linc-MD1 and muscle microRNAs (miR-206, miR-1 and miR-133) during *in vitro* C2 myoblast differentiation. The analysis reveals that: i) miR-206 is already expressed in GM (in line with the observed basal activity of the PROX promoter and its active chromatin signature, Figure 2A-C), ii) miR-1 and miR-133 expression is delayed with respect to miR-206 (note that the used probes do not allow us to distinguish between miR133a and miR-133b), iii) linc-MD1 expression starts from the third day of differentiation.

In order to understand the role of linc-MD1 in skeletal muscle differentiation, we modulated its expression through RNA interference and over-expression experiments. The left panel in Figure 4B shows that, in C2 myoblasts, the MYOG and MHC protein levels decrease after 5 days of linc-MD1 interference (si-MD1) with respect to control siRNA (si-scr).Two different constructs were used for ectopic expression of linc-MD1 (see scheme in Figure 4B): pMD1, carrying the linc-MD1 cDNA (Figure S1), and pMD1-Δdrosha, containing a mutation in the miR-133b flanking region that prevents Drosha cleavage and miR-133b release. The use of both constructs should permit to distinguish the effect of linc-MD1 from that of miR-133b that can be produced in the nucleus from Drosha cleavage of the linc-MD1 precursor. Figure S4 demonstrates that pMD1 is indeed able to express high levels of miR-133b, while pMD1-Δdrosha is not. Figure 4B (right panel) shows that both types of constructs give rise to an increase of myogenic markers, MyoG and MHC, with respect to control treatment (pCtrl). Interestingly, pMD1-Δdrosha displayed a slightly stronger activity (more evident for MHC), indicating that the observed effects are not due to miR-133b production but rather to linc-MD1 overdosage. Lower panels of Figure 4B indicate the relative quantification of linc-MD1 with respect to controls. Considering the disproportion between linc-MD1 abundance and the effects on myogenic target synthesis, it is reasonable to postulate the existence of a threshold level above which the system cannot be further influenced.

linc-MD1 is a target of miR-133 and miR-135

Bioinformatics analysis (see Supplemental Experimental Procedures) for miRNA recognition sequences on linc-MD1 revealed the presence of thirty-six highly conserved putative miRNA sites listed in Supplementary Table I. We discarded miRNAs not expressed in muscle as well as miRNAs whose targets are not expressed or do not have a known function in muscle physiology. The two remaining miRNA were miR-135, with two predicted sites on linc-MD1 and miR-133, with one site (see Figure 5A and Supplementary Table I; note that both members, a and b, of the miR-135 and miR-133 families can associate with those sites on linc-MD1). Interestingly the 70 nucleotide shorter isoform of linc-MD1 (see Figure 1C) lacks the two miR-135 sites. In all subsequent experiments we concentrated on the longest isoform containing the miR-135 sites (linc-MD1 cDNA).

The linc-MD1 cDNA (RLuc-MD1-WT) and mutant derivatives lacking the putative miR-135 and miR-133 recognition sequences (RLuc-MD1-Δ135 and RLuc-MD1-Δ133) were cloned

downstream of the luciferase gene (Figure 5B) and transfected in C2 myoblasts together with either miR-135 (pmiR-135a/b) or miR-133 (pmiR-133a/b) coding plasmids. Figure 5B shows that luciferase expression is reduced by 50% and 20% with respect to the control plasmid (pCtrl) when miR-135 and mir-133 were expressed, respectively. These effects are abolished when mutant substrates for either miRNA were utilized. qRT-PCR for mRNA revealed that miR-135 and miR-133 do not affect luciferase mRNA stability (Figure S5A). These data demonstrate that linc-MD1 can bind both miR-135 and miR-133.
The different levels of repression exerted by the two miRNAs could be due to the fact that linc-MD1 contains two miR-135 recognition elements and only one for miR-133. However, it cannot be excluded that the presence of a pre-miR-133b hairpin structure in the linc-MD1 sequence could limit miR-133 association.

linc-MD1 controls miR-133 and miR-135 targets

Among the many predicted targets of miR-135 and miR-133, we concentrated on MEF2C (with one miR-135 site) and MAML1 (with two miR-133b sites) mRNAs since they encode for transcription factors known to play a relevant role in myogenic differentiation (Shen et al., 2006). Interestingly, comparative analysis revealed that miRNA putative target sites in MEF2C and MAML1 3'UTR are highly conserved in mammals. The 3'UTRs of MAML1 and MEF2C were fused to the Luciferase coding region (RLuc-maml1-WT and RLuc-mef2c-WT, Figure 5C) and transfected in C2 myoblasts with plasmids encoding miR-135 (pmiR-135a/b) or miR-133 (pmiR-133a/b) in parallel to a control plasmid (pCtrl). Luciferase assays show that MAML1 and MEF2C are targets of miR-133 and miR-135, respectively (Figure 5C). The use of mutant derivatives (-*mut*) in the miRNA recognition sites confirms the specificity of the repressing activity. Moreover, LNA against miR-133 or miR-135 were able to prevent the repression by the endogenous miRNAs on RLuc-maml1-WT and RLuc-mef2c-WT, respectively (Figure S5B).
RLuc-maml1-WT and RLuc-mef2c-WT constructs were subsequently transfected in C2 myoblasts together with pMD1-ΔDrosha or mutant derivatives (pMD1-Δ135 and pMD1-Δ133; see Figure 5D). Luciferase assays indicate that, in the presence of the pMD1-ΔDrosha, both 3'UTR reporter constructs are up-regulated (Figure 5D, black bars). This indicates that linc-MD1, by binding miR-133 and miR-135, acts as a "decoy" abolishing miRNA repressing activity on both MAML1 and Mef2C 3'UTR. On the contrary, when the

pMD1-Δdrosha -Δ133 was used, RLuc-maml1-WT repression is restored, as it is also the case for pMD1-Δdrosha–Δ135 on RLuc-mef2c-WT (dotted and dashed bars respectively). These effects were lost when both RLuc-maml1-*mut* and RLuc-mef2C-*mut* were utilized.

Figure 6A shows MAML1 and MEF2C expression in parallel with that of miR-133 and miR-135 during C2 myoblasts differentiation. The effect of linc-MD1 on the MAML1 and MEF2C endogenous proteins in combination with a modulation of miRNA levels was monitored by different approaches shown in Figure 6B: i) LNA against miR-135 and 133b; ii) RNAi against linc-MD1; iii) RNAi against linc-MD1 in combination with LNA against miR-135 and 133b and iv) overexpression of linc-MD1 either in its wild-type form or in its Δdrosha mutant derivative. The results indicate that the levels of MAML1 and MEF2C increase in the presence of LNA against miR-135 and miR-133, while they decrease in the absence of linc-MD1. Notably LNA are able to resume synthesis of both proteins when linc-MD1 was downregulated by RNAi. Finally, the overexpression of linc-MD1 either in its wild-type form or in its Δdrosha mutant derivative produced a 1.5-1.9 fold increase of MAML1 and MEF2C expression. These data indicate the existence of a specific cross-talk between the linc-MD1 RNA and MAML1 and MEF2C mRNAs through competition for miR-133 and miR-135 binding.

If linc-MD1 effectively acts as a "decoy", one would expect that the relative concentration of the decoy and the miRNAs affects the expression of the target mRNAs. We gradually increased the amount of miRNAs in the presence of increasing amount of linc-MD1-Δdrosha. Figure 6C indicates that the levels of the endogenous MAML1 and MEF2C are higher in excess of linc-MD1 and are gradually reduced when miRNA levels are increased. This further proves that there is an interplay among the three components.
Since muscle creatine kinase (MCK) was previously shown to be controlled by MEF2C in concert with MAML1 (Shen et al., 2006), we tested the effect of linc-MD1 knock-down and overexpression on this downstream target. Figure 6D shows that the amount of MCK directly correlates with that of its transcriptional activators, demonstrating that the linc-MD1 and miR-135/133 circuitry indeed impinges on muscle gene expression.
Altogether these data indicate that linc-MD1, by binding miR-133 and miR-135, acts as a competing endogenous RNA (ceRNA) for their mRNA targets, including MAML1 and MEF2C, which encode crucial myogenic factors required for the activation of muscle-specific genes. Incidentally, in line with a "decoy" mechanism, the predicted ΔG of binding

(Enright et al,2003) of the miRNAs with linc-MD1 is lower than that with the respective targets (Figure S6).

The linc-MD1 function is conserved in human myoblasts

Taking advantage of the presence of conserved regions in linc-MD1, we amplified a linc-MD1 human homologue from differentiated primary myoblasts. We confirmed the exon/intron organization and, in particular, the conservation around the recognition motifs for miR-135 and miR-133. Human primary myoblasts were analyzed in parallel with Duchenne myoblasts (DMD), characterized by mutations in the dystrophin gene and known to have a reduced ability of undergoing terminal differentiation (Cacchiarelli et al., 2011). Figure 7A shows that, compared to control cells, DMD myoblasts display a reduced and delayed accumulation of the muscle-specific markers MyoG and MHC. Notably, in DMD cells the linc-MD1 levels are strongly reduced. This, together with the unaffected accumulation of miR-135, likely determines low levels of MEF2C; vice versa, the strong downregulation of miR-133 correlates with the upregulation of MAML1. The same results were also obtained during differentiation of satellite cells derived from wild-type and *mdx* animals (Figure S7).

Interestingly, when DMD myoblasts were infected with a lentiviral construct expressing the pMD1-Δdrosha, the expression levels of MyoG and MHC as well as those of MEF2C are restored towards control levels (Figure 7B). Despite the upregulation of miR-133, which parallels linc-MD1 overexpression, the MAML1 levels increase indicating that the amount of linc-MD1 is sufficient to overcome miR-133 repression activity.

In conclusion, these data indicate that also the human linc-MD1 RNA is able to modulate miR-133 and miR-135 targets and, in doing so, to play an important role in the timing control of myoblast differentiation.

DISCUSSION

It is becoming largely accepted that the non-coding portion of the genome rather than its coding counterpart is likely to account for the greater complexity of higher eukaryotes. Many new functions have been assigned to non-coding RNAs both in the nucleus and in the cytoplasm (Mattick, 2011; Nagano and Fraser, 2011). Likewise what happened for the well known small non-coding RNAs, long non-coding RNAs are now attracting much

interest. Recent data suggest that coding and non-coding RNAs can regulate one another through their ability to compete for microRNA binding; these molecules have been termed competing endogenous RNA (ceRNA, Salmena et al., 2011). ceRNAs can sequester microRNAs, thereby protecting their target RNAs from repression.
In this paper we identified a muscle specific long non-coding RNA (linc-MD1) which displays "decoy" activity for two specific miRNAs and, in doing so, regulates their targets in a molecular circuitry affecting the differentiation program.

We show that linc-MD1 is encoded by a genomic locus containing the miR-206 and miR-133b coding regions and demonstrate that there is a complex architecture in terms of transcriptional control in this locus: while miR-206 is expressed autonomously from its own proximal promoter, miR-133b is co-transcribed with linc-MD1 RNA which derives from a 13 Kb distal promoter.
We provide several evidence of the existence of two distinct promoters: i) miR-206 is already expressed in growing myoblasts while miR-133b and linc-MD1 are activated only upon differentiation; ii) 5' race and promoter fusion experiments indicated the existence of two transcriptional regulatory elements (DIST and PROX); iii) ChIP experiments for RNA Polymerase II and different markers of chromatin activity indicated a well defined chromatin organization of the two transcriptional units. In particular, in growth conditions, only the PROX promoter displayed markers of activation and no RNA PolII loading was detected on the miR133b region. These data suggest that miR-133b mainly originates from the DIST promoter by processing of linc-MD1.
linc-MD1 accumulates as a cytoplasmic poly-A+ RNA, supporting the conclusion that this species is the remaining portion of the transcript that escaped Drosha cleavage inside the nucleus. We proved that indeed miR-133b is produced when ectopically expressing linc-MD1. In order to avoid a possible confusion between the effect of linc-MD1 and of the released miR-133b in most of the over-expression experiments performed a mutant derivative lacking the ability to release miR-133b was utilized. Future work will address the mechanism regulating the relative ratio between miR-133b processing and the export of the unprocessed precursor.

Notably, we showed that transcriptional activation of the linc-MD1 promoter correlates with a DNA looping in which the distal and proximal promoters (and the polyadenylation region) are connected in a functional/structural interaction. Gene loops have so far been shown to

be transcription-dependent, as they are absent in non-transcribing conditions and have been suggested to represent specific structural domains of active chromatin (Tan-Wong et al., 2008; West and Fraser, 2005). Therefore, a drastic structural change occurs in the miR-206/miR-133b locus; in growth conditions only the miR-206 promoter is active and no long-distance interactions occur, while, upon differentiation, looping occurs between distantly located regions of the molecule and this correlates with activation of the distal promoter and consolidation of the overall transcription of the locus.

As far as the function of linc-MD1 is concerned, we showed that its modulation impinged on myogenesis. linc-MD1 RNAi-dependent down-regulation in mouse myoblasts produced a decrease in the accumulation of myogenic markers, while its over-expression led to increased synthesis. linc-MD1 was found to be conserved in human cells: high levels were observed upon induction of differentiation in wild-type cells while strongly reduced levels were found in Duchenne myoblasts. This observation is in line with the well known delay observed in the differentiation programme of DMD myoblasts (Cacchiarelli et al., 2011). Notably, when linc-MD1 expression was restored to wild-type levels in DMD myoblasts, the timing and expression level of the myogenic factors was partially rescued towards wild-type levels.

According to the ceRNA hypothesis, lncRNAs may elicit their biological activity through their ability to act as endogenous decoys for microRNAs; such activity would in turn affect the distribution of miRNAs on their targets (Salmena et al., 2011). We searched miRNA recognition motifs in the linc-MD1 sequence and found that the presence of recognition sites for miR-133 and miR-135 could be reliably predicted. linc-MD1 was validated as target for both these miRNAs since, in their presence, it induced translational repression of a reporter gene.

Among the many different putative targets for these miRNAs, we discovered two mRNAs encoding for proteins with a relevant function in myogenesis: the Myocyte-specific enhancer factor 2C (MEF2C) targeted by miR-135 and MAML1 controlled by miR-133.

Consistently with linc-MD1 being a decoy for miR-133 and miR-135, we proved that its depletion reduced the levels of both MAML1 and MEF2C, while its overexpression produced an increase in protein accumulation. These data are consistent with the idea that decoy lincRNAs are *trans* modulators of gene expression through microRNA binding.

The identification of the targets indirectly controlled by linc-MD1 can be instrumental to explain the myogenic alterations observed upon its deregulation. MEF2C belongs to a family of transcription factors that bind the control regions of numerous muscle-specific genes activating their expression (Lin et al., 1997). Mutations of the D-mef2 gene in D*.melanogaster* identified MEF2 as an essential cofactor for differentiation of skeletal, cardiac, and visceral muscle cells (Lilly et al., 1995). MEF2C was shown to regulate the M-line-specific proteins myomesin and M protein myomesin gene transcription, suggesting a key role for this factor in maintenance of sarcomere integrity and postnatal maturation of skeletal muscle (Potthoff et al., 2007).

On the other side the Mastermind-like (MAML) genes encode critical transcriptional co-activators for Notch signaling. Additionally, the MAML proteins were described as transcriptional co-activators in other signal transduction pathways including muscle differentiation: mice with a targeted disruption of the MAML1 gene had severe muscular dystrophy and MAML1-null embryonic fibroblasts failed to undergo MyoD-induced myogenic differentiation (Shen et al., 2006). Moreover, ectopic MAML1 expression in mouse myoblasts dramatically enhanced myotube formation and increased the expression of muscle-specific genes, while MAML1 knockdown inhibited differentiation.
Even more interesting is the finding that MAML1 and MEF2C specifically interact and act synergistically to activate several genes required for muscle development and function, including muscle creatine kinase. The MAML1 promyogenic effects were completely blocked upon activation of Notch signaling, which was associated with recruitment of MAML1 away from MEF2C to the Notch transcriptional complex (Wilson-Rawls et al., 1999). Therefore, a cross-talk between MAML1 and Notch was postulated to influence myogenic differentiation.

In light of these notions, we proved that depletion of linc-MD1 led to repression of both MAML1 and MEF2C, while its over-expression restored their synthesis at high levels. Notably, in conditions of linc-MD1 excess, titrated repression of both MAML1 and MEF2C could be obtained by increasing miR-133 and miR-135 levels. This indicated a direct competition for miRNA binding between linc-MD1 and mRNAs, allowing us to conclude that the three components cross-talk with one another at the post-trascriptional level. Notably, MCK, a known target of MEF2C, coherently behaved as part of the circuitry: it

increased upon linc-MD1 over-expression and decreased upon RNAi.

In Duchenne muscles the rescue of linc-MD1 through lentiviral-mediated expression produced the recovery of both MAML1 and MEF2C synthesis and partial rescue of the correct timing of the differentiation programme. These data allowed us to conclude, that also long non-coding RNAs play a relevant role in the complex network of regulatory interactions governing muscle terminal differentiation. Moreover, the discovery of the "decoy" role of lncRNA opens the road to the prediction and identification of new regulatory networks acting through microRNA competition.

EXPERIMENTAL PROCEDURES

Cell cultures and treatments

C2 myoblasts (C2.7 clone) were transfected with plasmid DNA using lipofectamine-2000. (Invitrogen). siRNA molecules designed against linc-MD1 exon2 and exon3 sequences (see supplementary experimental procedures) where transfected using HiPerfect (QIAGEN). LNA oligos against miR-133a/b and miR-135a/b (EXIQON) were transfected using XtremeGene (Roche). All transfections were performed according to manufacturer's specifications.

Control and Duchenne primary myoblasts carrying exon 44 deletion (obtained from Telethon Biobank), were grown and infected with lenti-Ctrl and lenti-MD1 constructs according to Incitti et al. (2010). Muscle satellite cells were cultured and differentiated as described in Cacchiarelli et al. (2010).

Chromatin Immunoprecipitation Assays

ChIP analyses were performed on chromatin extracts from myoblasts (GM) and myotubes (DM) according to manufacturer's specifications (MAGnify ChIP - Invitrogen) with the following antibodies: RNA Polymerase II, MyoD (Santa Cruz), anti-acetyl-HistoneH3 (Lys9), anti-acetyl-HistoneH3 (Lys4), anti-trimethyl Histone H3 (Lys27) (Millipore).

A standard curve was generated for each primer pair testing 5-point dilutions of input sample. Fold antibody enrichment was quantified using qRT-PCR (QuantiTect SYBR Green - QIAGEN) and calculated as a percent of input chromatin (% inp). Data were

normalized to an unrelated genomic region and are representative of three independent experiments. Primer sequences are available upon request.

3C analysis

The 3C assay was performed as described by Tan-Wong et al. 2008. Briefly, chromatin was crosslinked with 1% formaldehyde and nuclei were isolated by using Nonidet P-40. DNA was digested with 800 units of StyI restriction enzyme and ligated in 1X ligation buffer (NEB). Ligation products were purified using QIAquick PCR purification kit (QIAGEN). Two types of controls were included in the analysis. First, to ensure that primer efficiency does not introduce bias, a control template was generated by digesting and ligating equimolar amounts of all possible PCR products and used to calculate amplification efficiency of each primer pairs. Second, a loading control was generated by amplifying part of HPRT promoter to evaluate total amount of DNA used in the 3C analysis. We confirmed that all 3C primers amplified an artificial control template but not undigested and ligated, or digested but not ligated chromatin. Therefore we verified that the sequence of all 3C products was correct (not shown).

3C products detection was done in triplicate by GoTaq qPCR (Promega) according to manufacturer's instructions. Data were analyzed according Abou El Hassan and Bremner, (2009). Primer sequences are available upon request.

SUPPLEMENTAL INFORMATION

Supplemental information includes extended experimental procedures, 7 figures and 1 table.

ACKNOWLEDGMENTS

We thank N. Proudfoot and K. Perkins for introducing MC to the 3C analysis, M. Mora and the Telethon Neuromuscular Biobank for providing material and M. Marchioni for technical support. DC is a recipient of a Microsoft research PhD fellowship. This work was partially supported by grants from: Telethon (GGP07049), Parent Project Italia, EU project SIROCCO (LSHG-CT-2006-037900), KAUST KUK-I1-012-43, AIRC, IIT "SEED", FIRB, PRIN and BEMM.

REFERENCES

Abou El Hassan, M., and Bremner, R. (2009). A rapid simple approach to quantify chromosome conformation capture. Nucleic Acids Res. *37*, e35

Amaral, P.P. and Mattick, J.S. (2008). Noncoding RNA in development. Mamm. Genome 19, 454–492. Genome Res. *17*, 556–565.

Ballarino, M., Pagano, F., Girardi, E., Morlando, M., Cacchiarelli, D., Marchioni, M., Proudfoot. N.J., and Bozzoni, I. (2009) Coupled RNA processing and transcription of intergenic primary microRNAs. Mol Cell Biol. *29*, 5632-8.

Beltran, M., Puig, I., Peña, C., García, J.M., Alvarez, A.B., Peña, R., Bonilla, F., and de Herreros, A.G. (2008). A natural antisense transcript regulates Zeb2/Sip1 gene expression during Snail1-induced epithelial-mesenchymal transition. Genes Dev. *22*, 756-69.

Buckingham, M., and Vincent, S.D. (2009). Distinct and dynamic myogenic populations in the vertebrate embryo. Curr Opin Genet Dev. *19*, 444-53.

Cacchiarelli, D. et al. (2010). MicroRNAs involved in molecular circuitries relevant for the Duchenne muscular dystrophy pathogenesis are controlled by the dystrophin/nNOS pathway. Cell Metab. *12*, 341-351.

Cacchiarelli, D., Incitti, T., Martone, J., Cesana, M., Cazzella, V., Santini, T., Sthandier, O., and Bozzoni, I. (2011). miR-31 modulates dystrophin expression: new implications for Duchenne muscular dystrophy therapy. EMBO Rep. *12*, 136-141.

Cacchiarelli, D., Legnini, I., Martone, J., Cazzella, V., D'Amico, A., Bertini, E., and Bozzoni, I. (2011). miRNAs as serum biomarkers for Duchenne muscular dystrophy. EMBO Mol Med. *3*, 258-265.

Chaumeil, J., Le Baccon, P., Wutz, A., and Heard, E. (2006). A novel role for Xist RNA in the formation of a repressive nuclear compartment into which genes are recruited when silenced. Genes Dev. *20*, 2223–2237.

Chargé, S.B., and Rudnicki, M.A. (2004). Cellular and molecular regulation of muscle regeneration. Physiol Rev. *84*, 209-38

Chen, J.F., Mandel, E.M., Thomson, J.M., Wu, Q., Callis, T.E, Hammond, S.M., Conlon, F.L., and Wang, D.Z. (2006). The role of microRNA-1 and microRNA-133 in skeletal muscle proliferation and differentiation. Nat Genet. *38*, 228-233.

Eisenberg, I., et al. (2007). Distinctive patterns of microRNA expression in primary muscular disorders. Proc Natl Acad Sci. *104*, 17016-17021.

Enright, A.J., John, B., Gaul, U., Tuschl, T., Sander, C. and Marks, D.S. (2003). MicroRNA targets in Drosophila. Genome Biology *5* , R1.

Ginger, M.R., Shore, A.N., Contreras, A., Rijnkels, M., Miller, J., Gonzalez- Rimbau, M.F. and Rosen, J.M. (2006). A noncoding RNA is a potential marker of cell fate during mammary gland development. Proc. Natl. Acad. Sci. USA *103*, 5781–5786.

Gong, C., and Maquat, L.E. (2011). lncRNAs transactivate STAU1-mediated mRNA decay by duplexing with 3' UTRs via Alu elements. Nature *470*, 284-8.

Incitti, T., De Angelis, F.G., Cazzella, V., Sthandier, O., Pinnarò, C., Legnini, I., and Bozzoni, I. (2010). Exon skipping and Duchenne Muscular Dystrophy therapy: Selection of the most active U1 snRNA-antisense able to induce dystrophin exon 51skipping. Mol. Ther. *18*,1675-1682

Khaitan, D., Dinger, M.E., Mazar, J., Crawford, J., Smith, M.A., Mattick, J.S. and Perera, R.J. (2011). The melanoma-upregulated long noncoding RNA SPRY4-IN1 modulates apoptosis and invasion. Cancer Res., *71*, 3852-62

Lilly, B., B. Zhao, G. Ranganayakulu, B. M. Paterson, R. A. Schulz, and E. N. Olson. (1995). Requirement of MADS domain transcription factor D-MEF2 for muscle formation in Drosophila. Science *267*, 688–693.

Lin, Q., Schwarz, J., Bucana, C., and Olson, E.N. (1997). Control of mouse cardiac morphogenesis and myogenesis by transcription factor MEF2C. Science *276*, 1404-7.

Loewer, S. et al. (2010). Large intergenic non-coding RNA-RoR modulates reprogramming of human induced pluripotent stem cells. Nat. Genet. *42*, 1113–1117.

McCarthy JJ. (2008). MicroRNA-206: the skeletal muscle-specific myomiR. Biochim Biophys Acta *1779,* 682-91.

Mattick J.S. (2011). The central role of RNA in human development and cognition. FEBS Letters *585*, 1600–1616.

Moore, M.J. and Proudfoot, N.J. (2009). Pre-mRNA processing reaches back to transcription and ahead to translation. Cell *136,* 688-700.

Nagano, T., and Fraser, P. (2011). No-nonsense functions for long noncoding RNAs. Cell. *145*, 178-81.

Okitsu, C.Y., Hsieh, J.C., and Hsieh, C.L. (2010). Transcriptional activity affects the H3K4me3 level and distribution in the coding region. Mol Cell Biol. *30,* 2933-46.

Poliseno, L., Salmena, L., Zhang, J., Carver, B., Haveman, W.J., and Pandolfi, P.P. (2010) A coding-independent function of gene and pseudogene mRNAs regulates tumour biology. Nature. *465*,1033-8.

Potthoff, M.J., Arnold, M.A., McAnally, J., Richardson, J.A., Bassel-Duby, R., and Olson, E.N. (2007). Regulation of skeletal muscle sarcomere integrity and postnatal muscle function by Mef2C. Mol Cell Biol. *27*, 8143-51.

Qureshi, I.A., Mattick, J.S., and Mehler, M.F., (2010). Long non-coding RNAs in nervous system function and disease. Brain Res. *18*, 20-35.

Rao, P.K., Kumar, R.M., Farkhondeh, M., Baskerville, S., and Lodish, H.F. (2006). Myogenic factors that regulate expression of muscle-specific microRNAs. Proc Natl Acad Sci U S A *103,* 8721-8726.

Rinn, J.L. et al. (2007). Functional demarcation of active and silent chromatin domains in human HOX loci by noncoding RNAs. Cell *129*, 1311–1323.

Salmena, L., Poliseno, L., Tay, Y., Kats, L., and Pandolfi, P.P. (2011) The *ceRNA* hypothesis: the Rosetta stone of a hidden RNA language. Cell, *in press* doi:10.1016 /j.cell.2011.07.014

Shen, H., McElhinny, A.S., Cao, Y., Gao, P., Liu, J., Bronson, R., Griffin, J.D., and Wu, L. (2006). The Notch coactivator, MAML1, functions as a novel coactivator for MEF2C-mediated transcription and is required for normal myogenesis. Genes Dev. *20*, 675-88.

Sleutels, F., Zwart, R. and Barlow, D.P. (2002). The non-coding Air RNA is required for silencing autosomal imprinted genes. Nature *415*, 810–813.

Tan-Wong, S.M., French, J.D., Proudfoot, N.J., and Brown, M.A. (2008) Dynamic interactions between the promoter and terminator regions of the mammalian BRCA1 gene. Proc Natl Acad Sci U S A. *105*, 5160-5.

Tripathi, V., et al. (2010). The nuclear-retained noncoding RNA MALAT1 regulates alternative splicing by modulating SR splicing factor phosphorylation. Mol. Cell *39*, 925–938.

Yuasa, K., Hagiwara, Y., Ando, M., Nakamura, A., Takeda, S., and Hijikata, T. (2008). MicroRNA-206 is highly expressed in newly formed muscle fibers: implications regarding potential for muscle regeneration and maturation in muscular dystrophy. Cell Struct Funct. 33, 163-169

West, A. G., and Fraser, P. (2005). Remote control of gene transcription. Hum. Mol. Genet. *14 Spec No 1*, R101–R111

Williams, A.H., Valdez, G., Moresi, V., Qi, X., McAnally, J., Elliott, J.L., Bassel-Duby, R., Sanes, J.R., and Olson E.N. (2009). MicroRNA-206 delays ALS progression and promotes regeneration of neuromuscular synapses in mice. Science *326*, 1549-54.

Wilson-Rawls, J., Molkentin, J.D., Black, B.L., and Olson, E.N. (1999). Activated notch inhibits myogenic activity of the MADS-Box transcription factor myocyte enhancer factor 2C. Mol Cell Biol. *19*, 2853-62.

Zhao, Y., Samal, E., and Srivastava, D. (2005) Serum response factor regulates a muscle-specific microRNA that targets Hand2 during cardiogenesis. Nature. *436*, 214-20.

Figure 1. Muscle specific lincRNA profiling

A) Human miRNA genomic location relative to their host genes B) Schematic representation of the murine miR-206/133b genomic locus. *Upper panel*: transcriptional start sites (TSS, indicated by arrows) mapped through 5' RACE analysis in differentiated myoblasts are displayed. The genomic structure of the identified linc-MD1 and the exon-intron lengths are shown as well as pre-miRNA sequences. *Lower panel*: conserved regions among vertebrates are shown together with E-boxes and regulatory elements (DIST, PROX and pA-signals). C) RT-PCR for linc-MD1, pri-miR-206 and pri-miR-133b expression performed in mouse myoblasts in growth (GM) or differentiation (DM) conditions. The total, nuclear (nuc), cytoplasmic (cyt), polyadenylated (pA+) and non-polyadenylated (pA^-) RNA fractions are shown. The same analysis was also performed in primary satellite cells in GM and DM conditions and in mouse embryonic fibroblasts (MEFs) infected with a MyoD expressing lentivirus (MyoD) or control (gfp). HPRT mRNA was used as endogenous control. D) Northern blot analysis for linc-MD1 in the poly-A+ fraction from mouse myoblasts in GM and DM conditions. E) RT-PCR for linc-MD1, pri-miR-206, pri-miR-133b performed on RNA from liver (LIV), heart (HEA), tibialis anterior (TIB) and soleus (SOL) of wild-type (WT) and *mdx* mice. F) *In situ* analysis with a DIG-labelled linc-MD1 probe in C2 myoblasts in GM and DM. G) *In situ* analysis with DIG-labelled linc-MD1 and miR-206 probes in wild-type (WT) and *mdx* gastrocnemius cryosections; DAPI staining (light blue) is also shown. Original magnification X20, scale bar 100 μm. Additional fields and controls are show in Figure S2.

Figure 2. Transcriptional and epigenetic regulation of miR-206/133b genomic locus

A) Promoter activity assay. *Upper panel*: distal (box D) and proximal (box P) regions were cloned upstream of murine pre-miR-223 and tested in C2 myoblasts in GM and DM conditions. A region between miR-206 and miR-133b was used as negative control (dashed box). miR-223 expression was measured by Northern blot (Figure S3) and qRT-PCR. U6 snRNA was used as endogenous control. miR-223 relative quantification (RQ) is shown with respect to the value of the control vector in GM set to a value of 1. *Lower panel*: the same regions were cloned, alone or in combinations, in a firefly luciferase reporter construct (FLuc) and tested in GM and DM conditions. A luciferase construct

(RLuc) was transfected as control. Luciferase activity, from three independent experiments, was measured as FLuc/RLuc RQ shown with respect to the negative control vector in GM set to a value of 1. One asterisk: $p<0.05$, two asterisks: $p<0.01$. B) ChIP analysis for MyoD enrichment on distal (DIST), proximal (PROX) and negative control (CTRL) regions performed on chromatin extracted from C2 myoblasts in GM and DM conditions. Amplifications of IgG control immunoprecipitations (IgG) and 10% of input chromatin (Inp) are shown. C) *Upper panel*: schematic representation of the miR-206/133b genomic locus. Capital letters indicate regions analyzed in ChIP experiments. Location of regulatory regions (DIST, PROX and pA), pre-miRNAs (206, 133b) and linc-MD1 are shown along the locus as in Figure 1B. *Lower panel*: ChIP analyses for RNA polymerase II (RNAP II), H3K9Ac, H3K27me3 and H3K4me3 were performed on chromatin extracted from myoblasts in GM and DM. Values derived from three independent experiments were normalized for background signals (IgG) and expressed as percentage of Input chromatin (% Inp). Unless specifically indicated, statistical significance was calculated with respect to GM conditions. One asterisk: $p<0.05$; two asterisks: $p<0.01$.

Figure 3. Tri-dimensional architecture of miR-206/133b genomic locus

A) *Upper panel*: StyI restriction sites (vertical lines), regulatory regions (DIST, PROX, pA), pre-miRNAs (206, 133b) and linc-MD1. Capital letters (A-I, X and Y) indicate the position of StyI sites analyzed in 3C experiments. A-I sites identify the same regions analyzed in ChIP experiments in Figure 2C. A common reverse primer identifying the proximal region (X) was used in combination with different reverse primers. *Lower panel*: 3C analysis performed on chromatin extracted from C2 myoblasts in GM and DM conditions and from fibroblast cell cultures. Cross-linking frequencies relative to X region were measured both by semi-quantitative PCR (data not shown) and qRT-PCR. Data from multiple experiments were normalized for primer amplification efficiency and reported with respect to X-B interaction in GM set to a value of 1. Statistical significance was calculated with respect to GM conditions. B) The same 3C analysis was performed in liver (LIV), heart (HEA), tibialis anterior (TIB), soleus (SOL) of wild-type (WT) and *mdx* animals. For each set of interactions analyzed, cross-linking frequencies relative to X region derived from multiple experiments were reported with respect to WT HEA interaction set to a value of 1. Statistical significance was calculated with respect to WT HEA tissue. One asterisk:

p<0.05; two asterisks: p<0.01. C) Schematic representation of the interactions detected upon induction of differentiation.

Figure 4. Modulation of linc-MD1 expression affects myogenesis

A) RNA and protein samples were extracted from proliferating myoblasts (GM) and after shift to differentiation medium (DM) for the indicated times. *Upper panels:* Western blot analysis for myogenin (MYOG), myosin heavy chain (MHC) and HPRT. *Middle panels:* RT-PCR analysis for linc-MD1 and Actin mRNA (ACT) expression. *Lower panels:* Northern blots for miR-206, miR-1, miR-133 and snoRNA55. B) *Left panel:* siRNAs for linc-MD1 (si-MD1) or scramble controls (si-scr) were transfected in C2 myoblasts and maintained in DM for 5 days. *Right panel*: linc-MD1 overexpression was obtained by transfection of plinc-MD1 and plinc-MD1-Δdrosha constructs (see schematic representation below) together with a control GFP cDNA (pCtrl). Samples were collected 4 days after induction of differentiation. Densitometric analysis, normalized for HPRT, is shown below. *Lower panels:* the levels of linc-MD1, normalized for HPRT, measured by qRT-PCR. Data are shown with respect to control experiments set to a value of 1. One asterisk: p<0.05; two asterisks: p<0.01.

Figure 5. linc-MD1 acts as a natural decoy for miR-135 and miR-133

A) Positions of miR-135 and miR-133 binding sites on linc-MD1. B) linc-MD1 (pRLuc-MD1-WT) and mutant derivatives devoid of miR-135 or miR-133 binding sites (pRLuc-MD1-Δ135 and pRluc-MD1-Δ133) were cloned downstream the Renilla luciferase coding region (RLuc). These constructs were co-transfected in C2 myoblasts together with plasmids expressing miR-135 (pmiR-135a/b) or miR-133 (pmiR-133a/b) or with a control vector (pCtrl). C) The 3'UTR of MAML1 and of MEF2C were cloned downstream RLuc (RLuc-maml1-WT, RLuc-mef2c-WT) together with mutant derivatives lacking miRNA recognition sequences (RLuc-maml1-*mut* and RLuc-mef2c-*mut*). These constructs were co-transfected in C2 myoblasts with plasmids expressing miR-135 (pmiR-135a/b) or miR-133 (pmiR-133a/b) or with a control vector (pCtrl). D) RLuc-maml1-WT, RLuc-mef2c-WT and their corresponding mutant derivatives (-*mut*) were transfected in C2 myoblasts with pMD1-Δdrosha or its mutant derivatives depleted in either miR-135 (pMD1-Δdrosha-Δ135) or miR-133 (pMD1-Δdrosha-Δ133) recognition elements. A GFP construct was used as

control (pCtrl). For miRNA overexpression experiments, unless specifically stated, a mix of a and b pre-miRNA plasmids was used. For all the experiments, histograms indicate the values of luciferase measured 24 hours after transfection. Data, derived from three independent experiments, are shown with respect to the values of RLuc control vector set to a value of 100%. One asterisk: $p<0.05$; two asterisks: $p<0.01$.

Figure 6. linc-MD1 modulates MAML1 and MEF2C expression in muscle

A) Western blot analysis for MAML1, MEF2C and Muscle Creatine Kinase (MCK), in growth medium (GM) and at different days upon shift to differentiation conditions (DM). The relative expression of miR-133 and miR-135 is also reported. B) MAML1 and MEF2C levels upon modulation of miRNA and linc-MD1 levels in C2 myoblasts maintained in DM for 5 days. Modulation was obtained with: anti miR-133 and miR-135 LNAs, RNAi against linc-MD1, and linc-MD1 overexpression (pMD1 and pMD1-Δdrosha). Scrambled LNA and siRNAs were used as control. HPRT was used as a loading control. Below each panel, relative quantifications with respect to control samples set to a value of 1 are displayed. C) Western blot for the same proteins from C2 myoblasts transfected with different combinations of pMD1-Δdrosha and pmiR-135/pmiR-133 expressing plasmids. (+) corresponds to 1.5 μg pMD1-Δdrosha and to 50 ng of miR-135/miR-133, while (++) corresponds to 300 ng of pmiR-135/pmiR-133. Control myoblasts were transfected with 1.5 μg of a GFP plasmid (-). The values, derived from densitometric analysis, are reported with respect to mock samples set to a value of 1. In histograms, one asterisk: $p<0.05$. D) MCK measured in cells treated with the indicated LNA or siRNAs as in panel B).

Figure 7. linc-MD1 is conserved in human and it improves differentiation of Duchenne myoblasts

A) Myoblasts derived from healthy (Control) and Duchenne Muscular Dystrophy (DMD) individuals were induced to differentiate for the indicated times and RNA and protein samples were collected. Western blot analysis for the indicated proteins was performed in parallel with qRT-PCR for the expression of linc-MD1, miR-133 and miR-135. B) DMD myoblasts were infected with lentiviral vectors carrying a control GFP-expressing cassette (lenti-Ctrl) or the linc-MD1-Δdrosha construct under the control of the CMV promoter (lenti-MD1). Cells were induced to differentiate for the indicated times and RNA and protein

samples were collected. Western blot analysis for the indicated proteins was performed in parallel with qRT-PCR for the expression of linc-MD1, miR-133 and miR-135. C) Schematic representation of the circuitry linking linc-MD1, miR-135, miR-133 and muscle differentiation.

Figure 1

Click here to download high resolution image

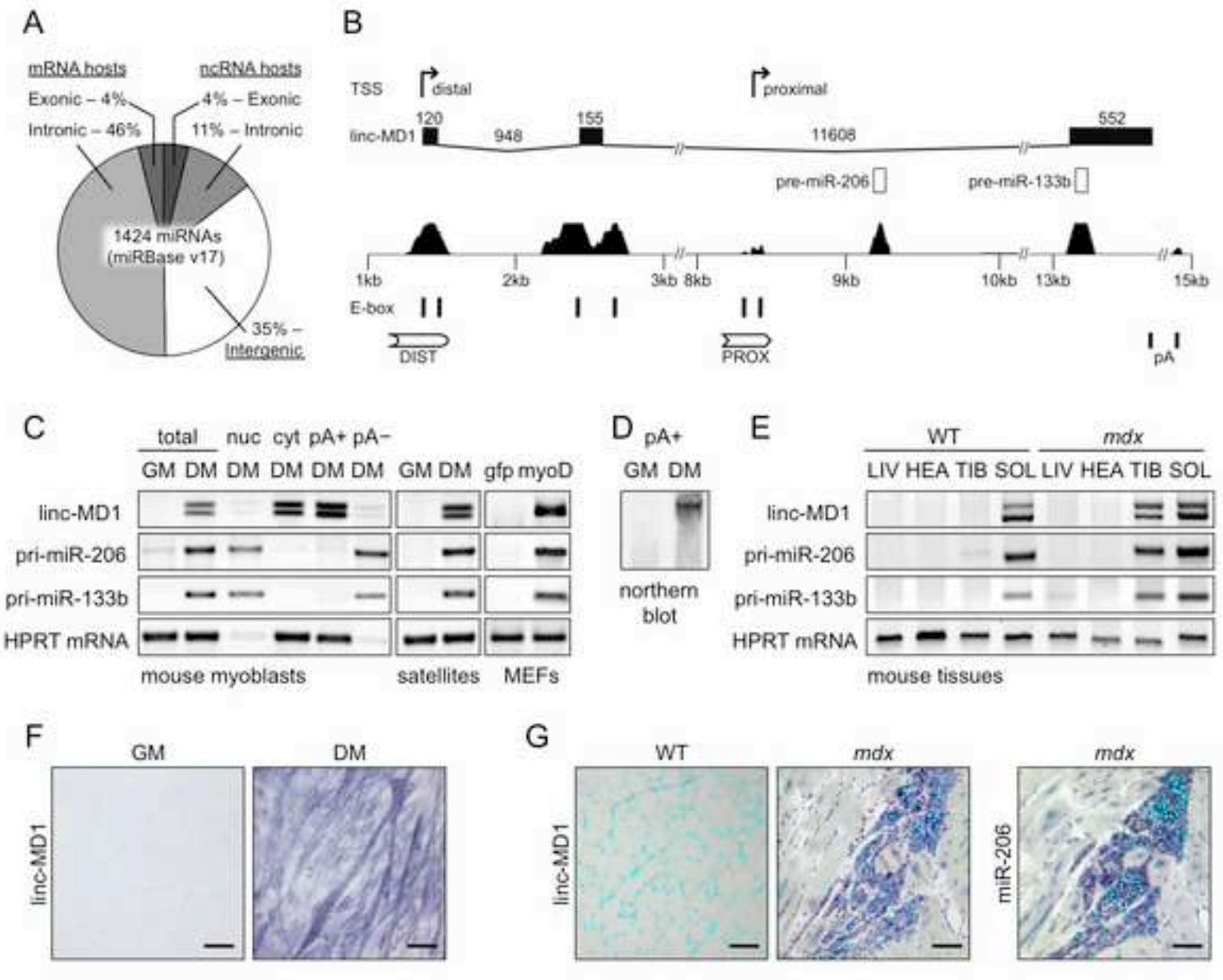

Figure 2

Click here to download high resolution image

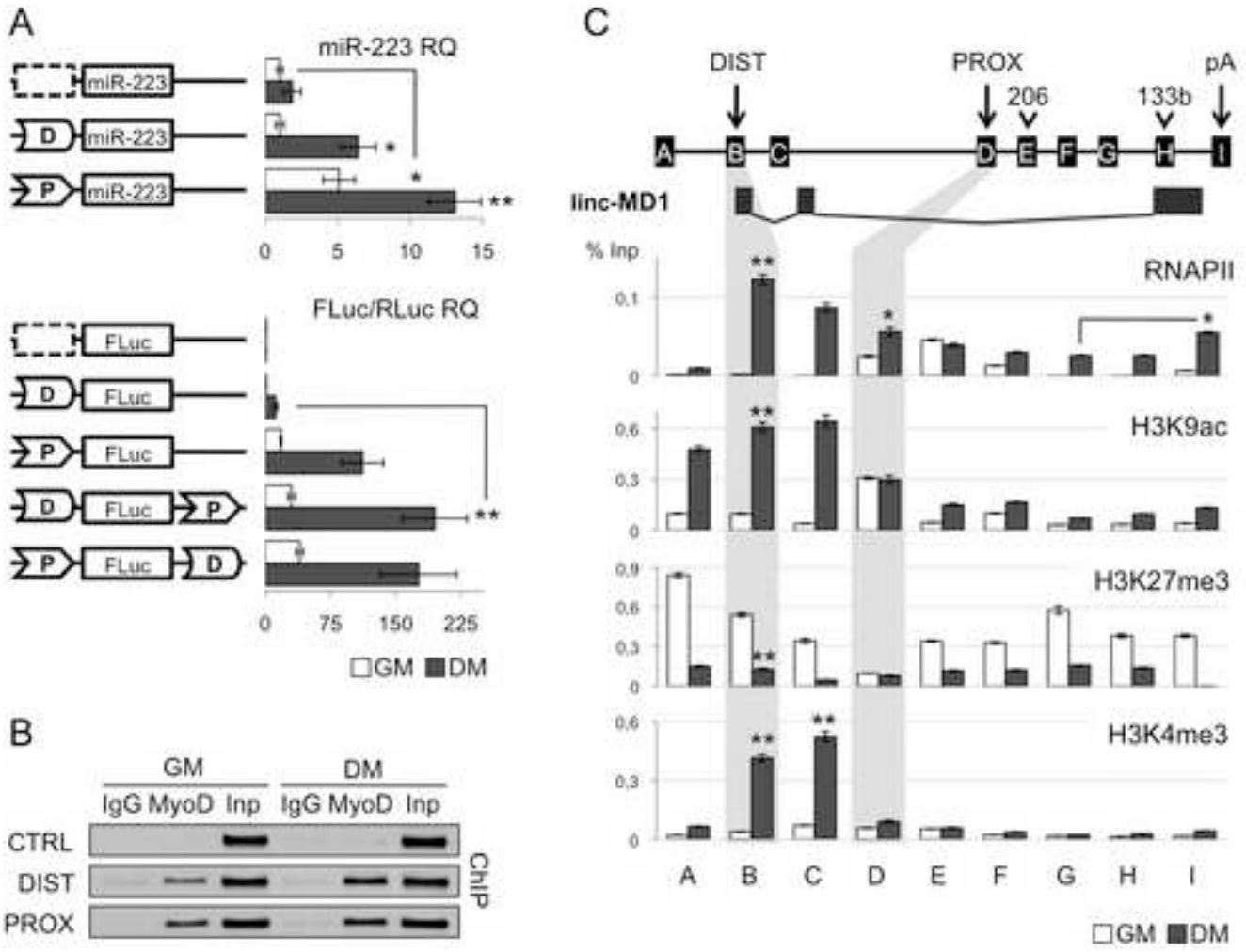

Figure 3

Click here to download high resolution image

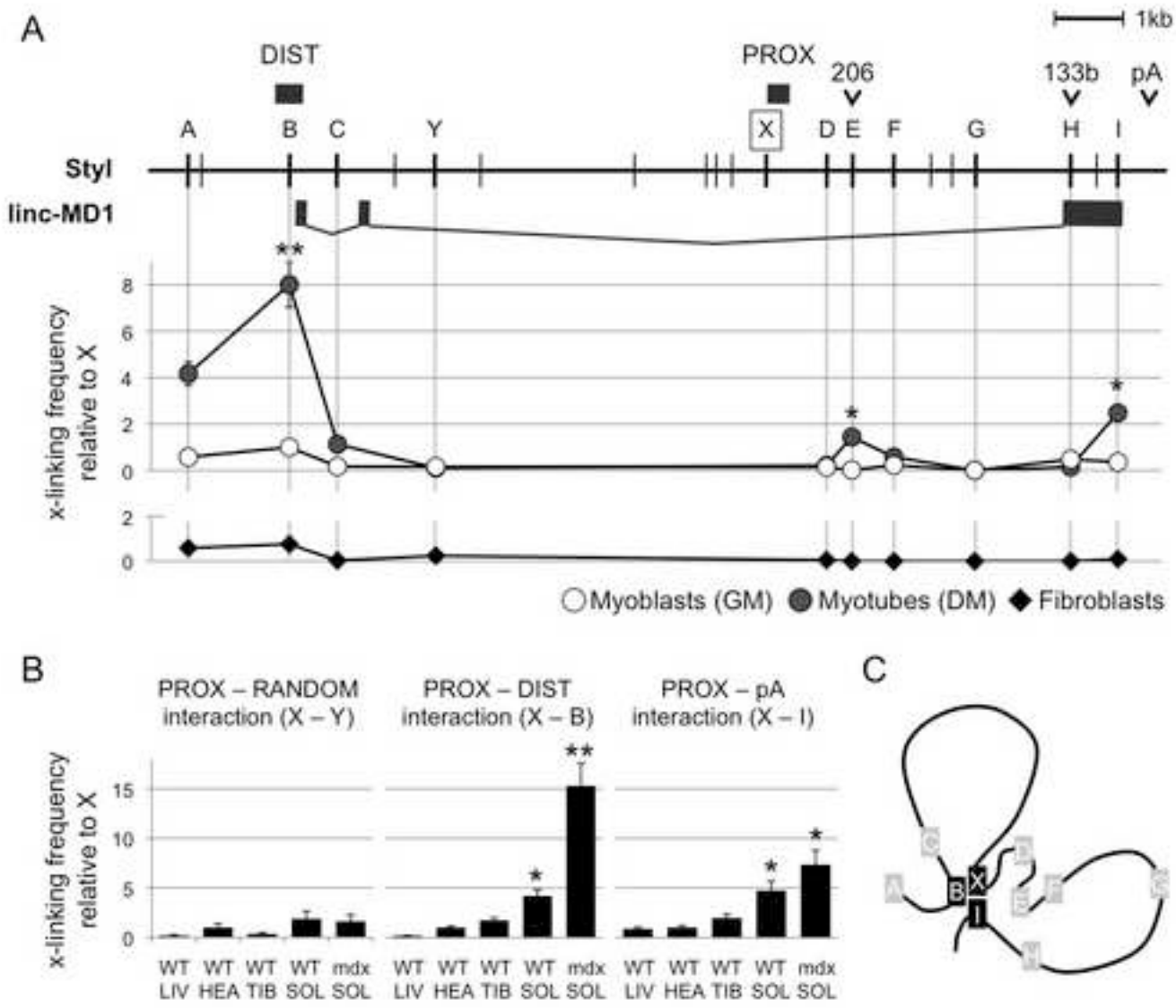

Figure 4

Click here to download high resolution image

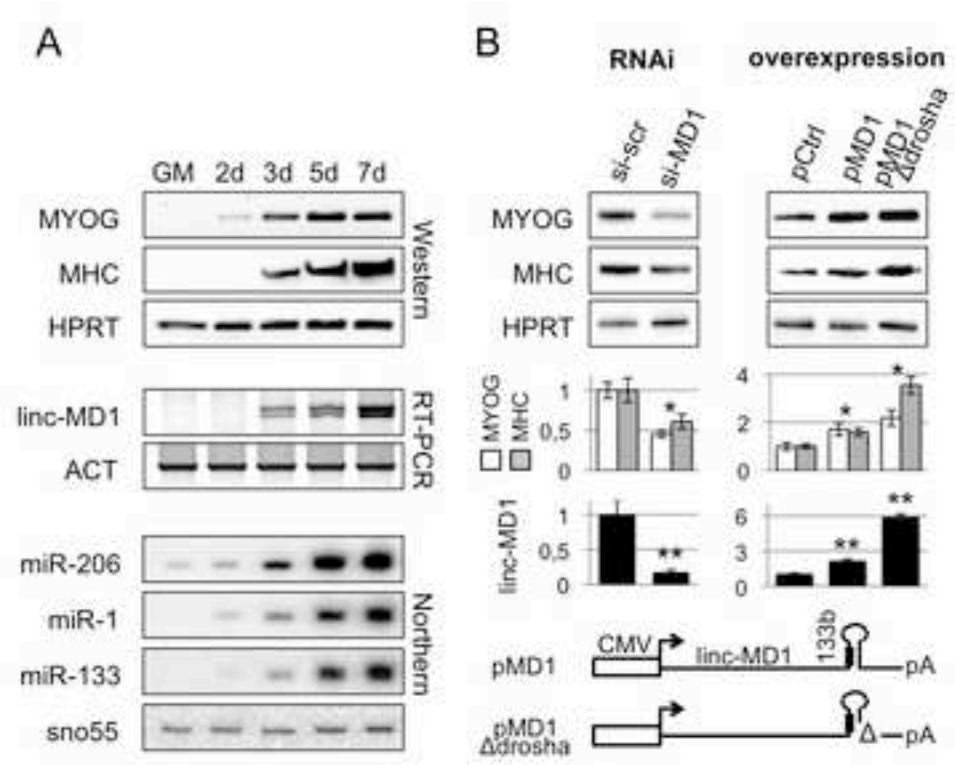

Figure 5

Click here to download high resolution image

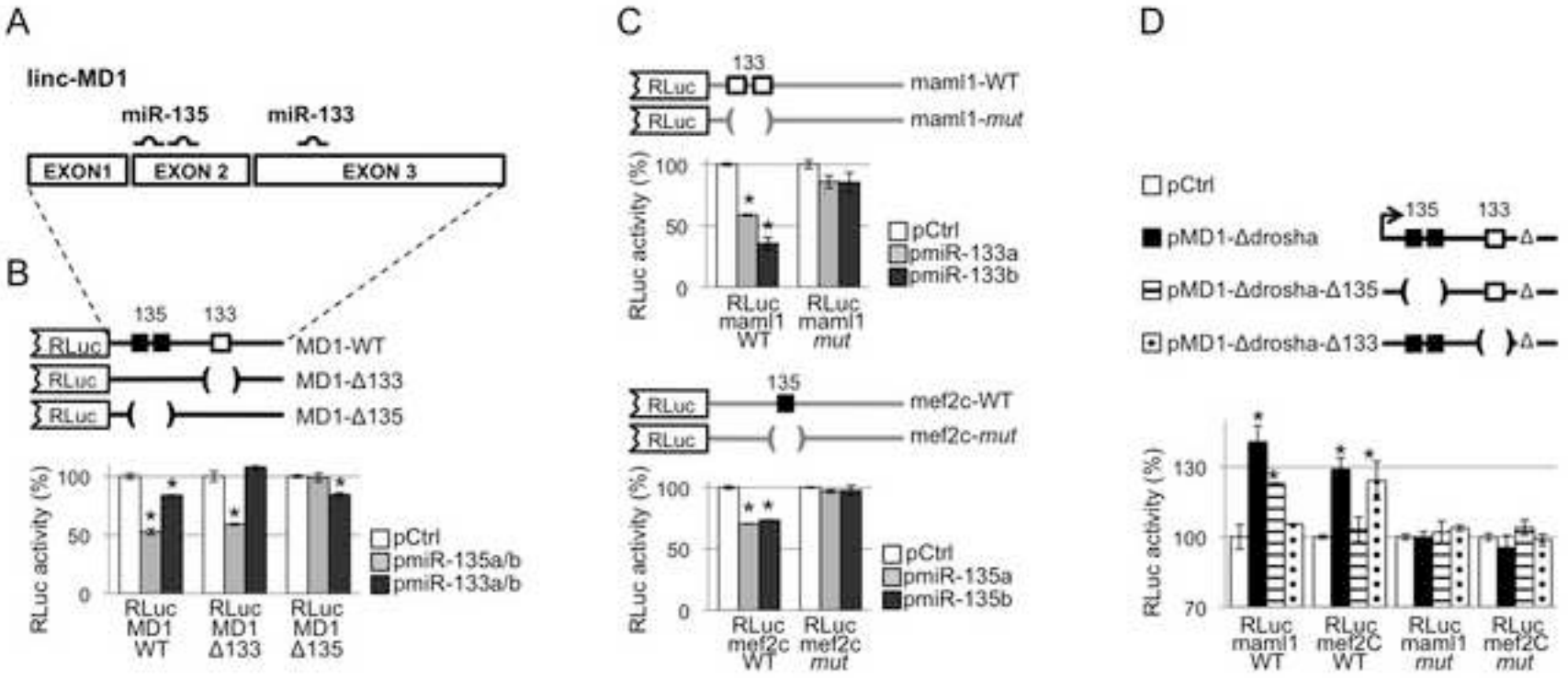

Figure 6

Click here to download high resolution image

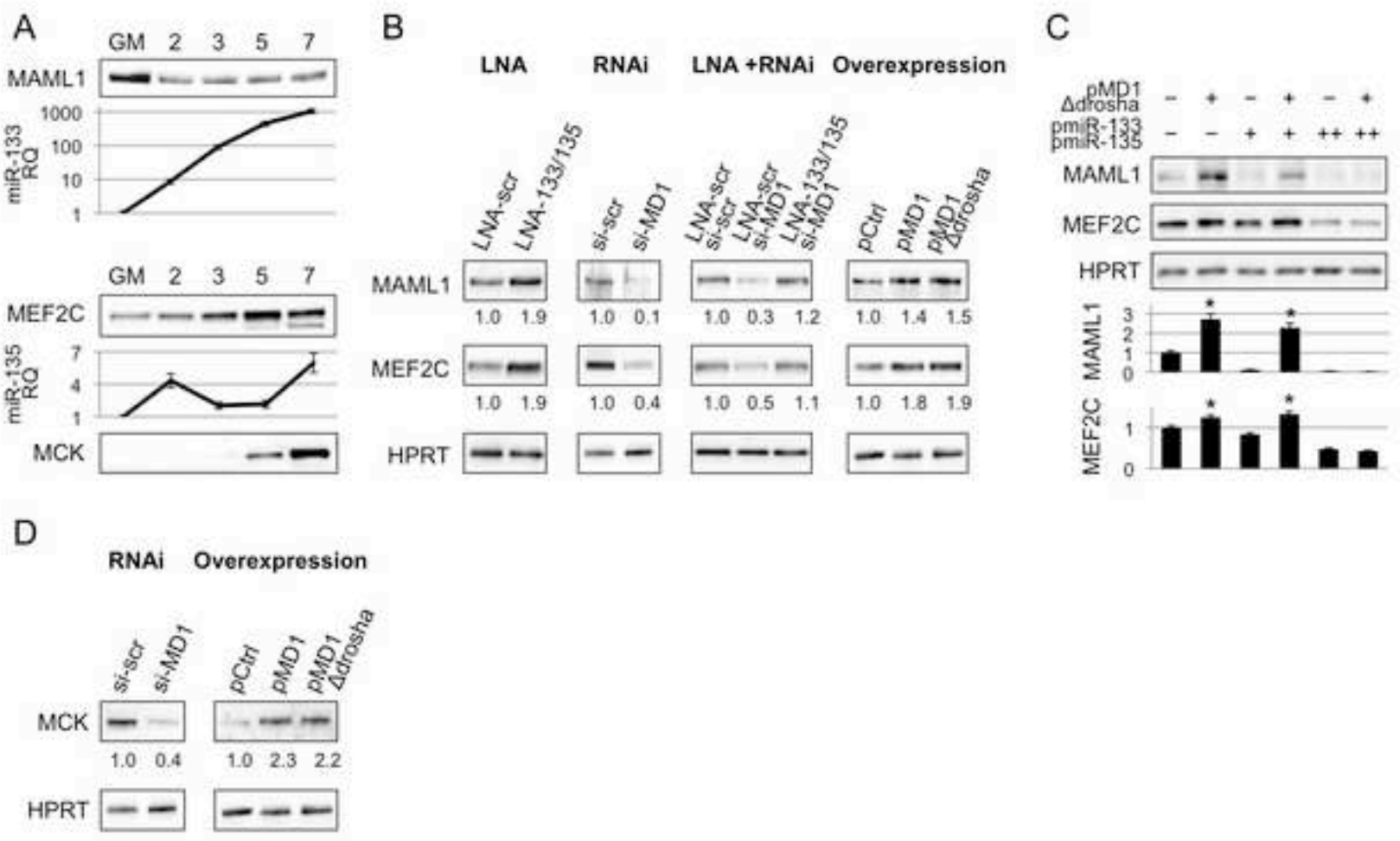

Figure 7

Click here to download high resolution image

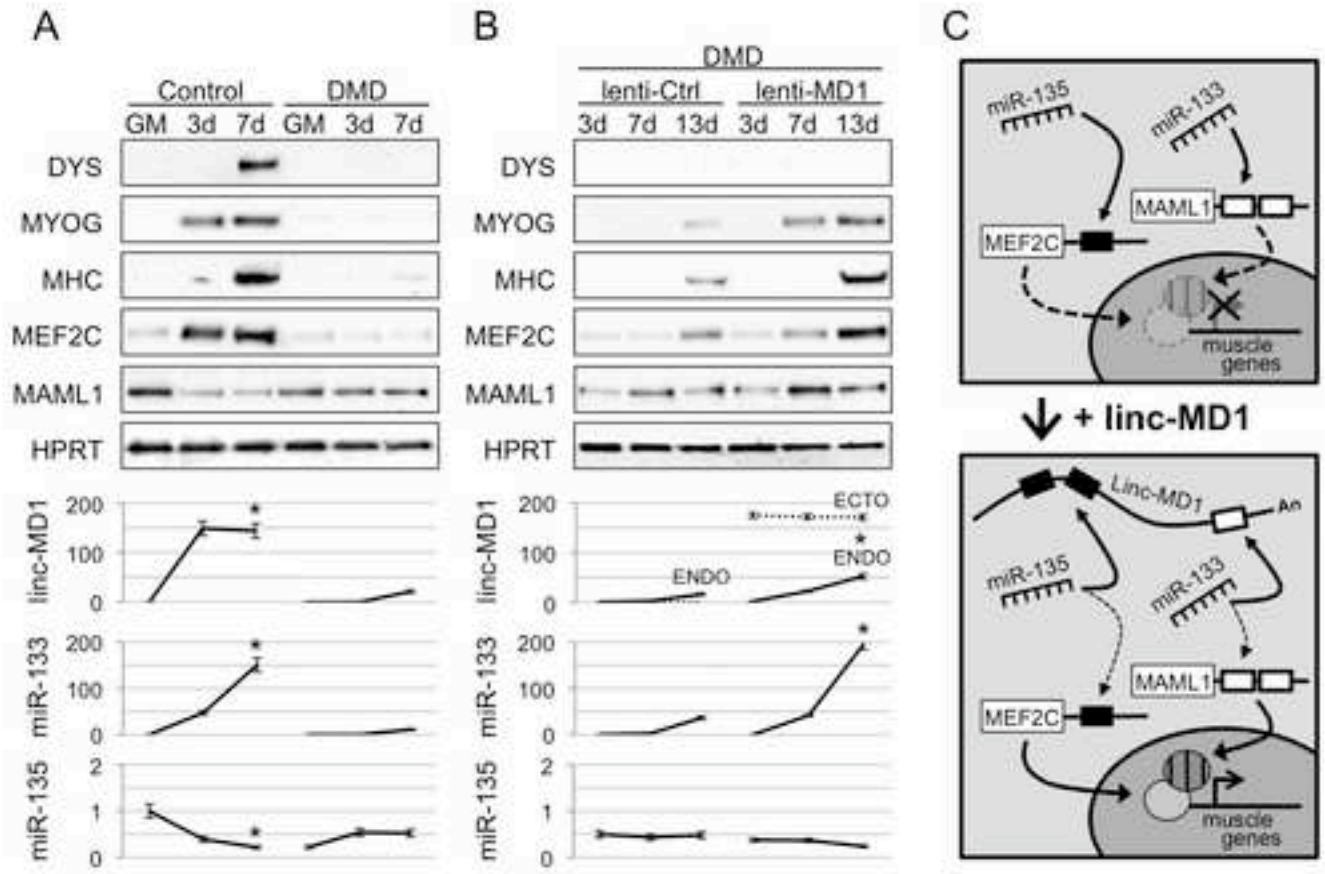

Inventory of Supplemental Information

Supplemental information includes extended experimental procedures, 7 figures and 1 table.

SUPPLEMENTAL FIGURES & TABLES

A

mmu-linc-MD1 (conserved exonic sequences)

```
  1  CTCTTTGCAGTGGGACAGCTGAAGAGGTATAATTTAACAGCTTTCAGAAG  50
 51  CCCGTCACTGGAGTGATTGAGGTGGACAGAAGGCAGGGACATGACCACGG 100
101  TCCTTAAAAGACACAAACAGGATTCTGACAGGAAGCCATAGAAATGCAAG 150
151  CCAACACTGCCAGCTCTGGAAATAAATAAATAATGACCCAGGTTCTATGC 200
201  TCCTCAATGGGGGCAGAAGCCTGCGGGGCAAGAAAACCACAGAGGAGGAG 250
251  GGACCTGCCTGCAACTTGTCCCCAGGCTTGGACAAGTGGTGCTCAAACTC 300
301  CAAGGACTTCACAAGCTTCAGGCTGCAGTCACCTCCAAAGGGAGTGGCCC 350
351  CCTGCTCTGGCTGGTCAAACGGAACCAAGTCCGTCTTCCTGAGAGGTTTG 400
401  GTCCCCTTCAACCAGCTACAGCAGGGCTGGCAAAGCTCAATATTTGGAGA 450
451  AAGAGAAGAGAAGAGAAAATAGCTGCTACAGCCTTGCTTATGAAAAGTAA 500
501  TGCTGGTTTTGCCATCATAGC..... 550
```

EXON1 – EXON2 – EXON3 – pre-miR-133b
AAGCCA – miR-135 seed
AACCAA – miR-133 seed
CCCCTTCAACCAGCTACAGCAGGG - Δdrosha deletion

B

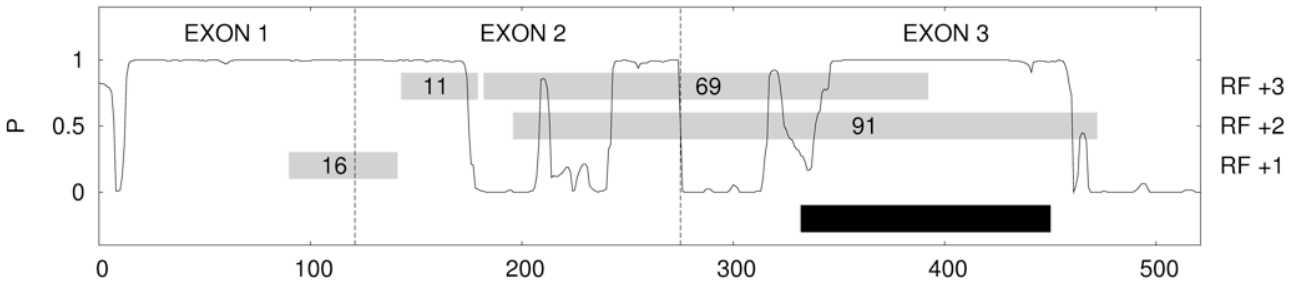

C

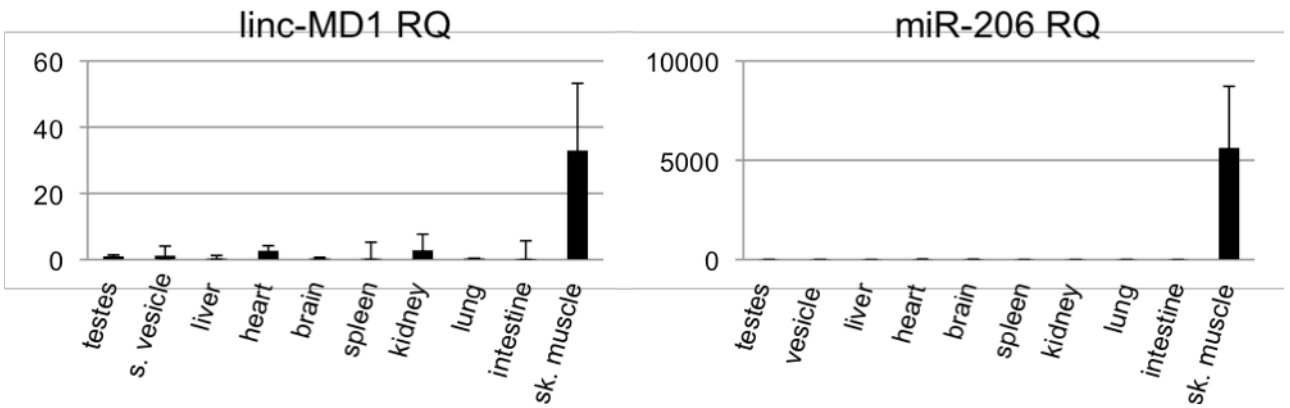

Figure S1

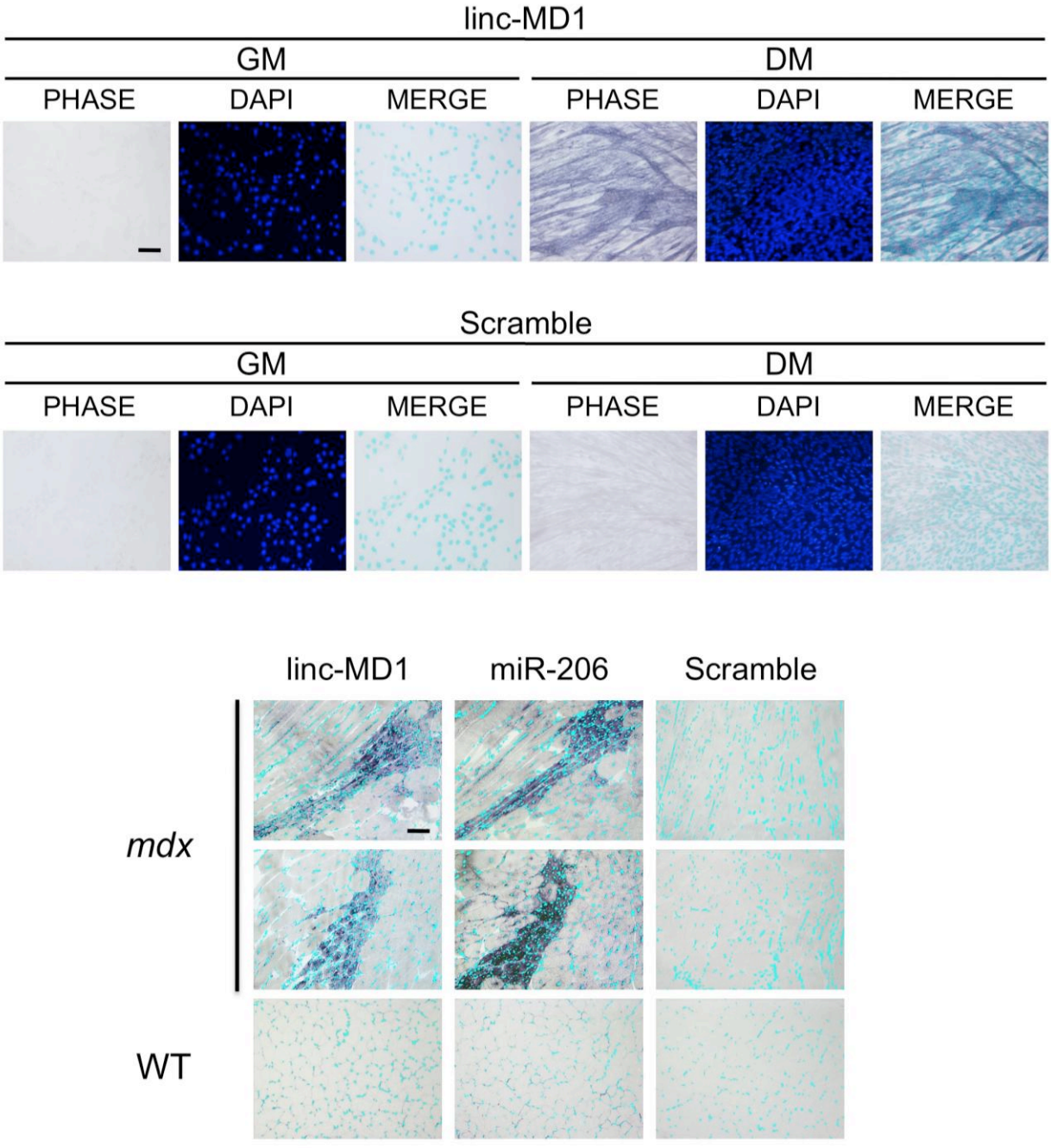
linc-MD1
GM
DM
PHASE
DAPI
MERGE
PHASE
DAPI
MERGE
Scramble
GM
DM
PHASE
DAPI
MERGE
PHASE
DAPI
MERGE
linc-MD1
miR-206
Scramble
mdx
WT

Figure S2

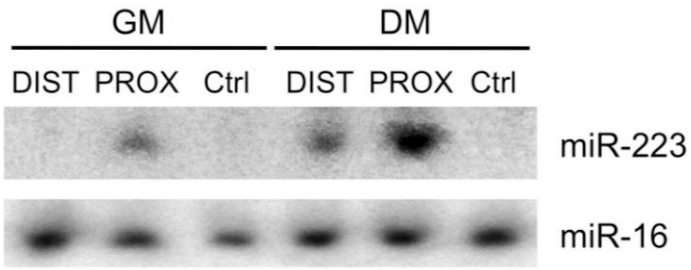

Figure S3

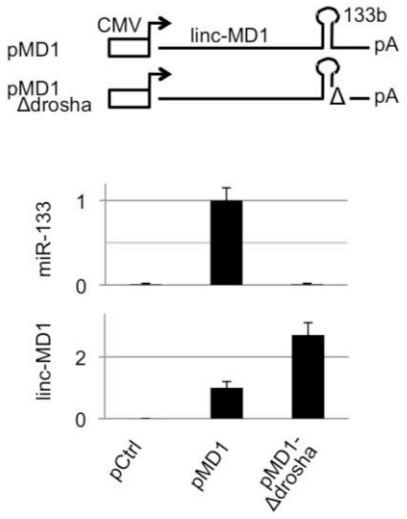

Figure S4

A

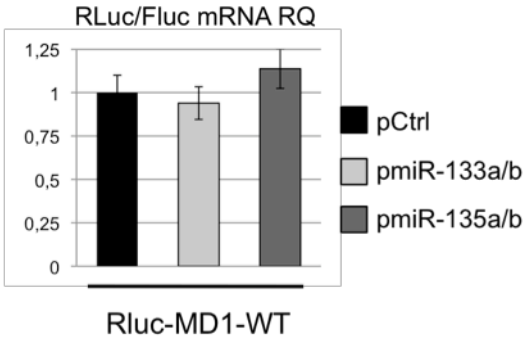

B

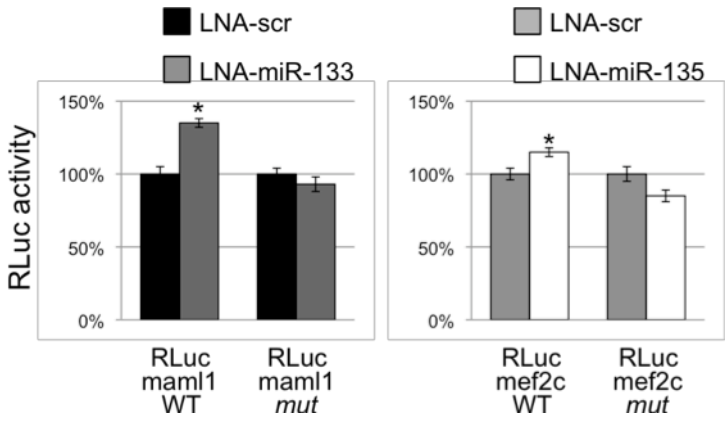

Figure S5

```
mmu-miR-135a :      3' AGUGUAUCCUUAUUUUUCGGUAU 5'
                        ||    | |  ||||||||
linc-MD1     :      5' CAGGAUUCUGACAGGAAGCCAUA 3'      ΔG: -16.37 kcal/mol

mmu-miR-135a :      3' AGUGUAUCCUUAUUUUUCGGUAU 5'
                       |||||  |||   ||||||
linc-MD1     :      5' AGCCAUAGAAAU-GCAAGCCAAC 3'      ΔG:-15.40 kcal/mol

mmu-miR-135a :      3' AGUGUAUCCUUAU--UUUUCGGUAU 5'
                         | | ||  | ||    ||||||||
Mef2c        :      5' AUAGAAAGCACUACCCUAAGCCAUG 3'    ΔG:-12.13 kcal/mol
-------------------------------------------------------------------------------

mmu-miR-135b :      3' AGUGUAUCCUUACUUUUCGGUAU 5'
                       |||||  ||||  ||||||
linc-MD1     :      5' AGCCAUAGAAAUG-CAAGCCAAC 3'      ΔG:-16.99 kcal/mol

mmu-miR-135b :      3' AGUGUAUCCU--UACU---UUUCGGUAU 5'
                         | | ||||   |||    ||||||||
linc-MD1     :      5' ACAAACAGGAUUCUGACAGGAAGCCAUA 3' ΔG:-18.78 kcal/mol

mmu-miR-135b :      3' AGUGUAUCCUUACUUUUCGGUAU 5'
                         | |     |    |||||||
Mef2c        :      5' AGAAAGCACUACCCUAAGCCAUG 3'      ΔG:-12.13 kcal/mol
-------------------------------------------------------------------------------

mmu-miR-133a :      3' GUCGACCAACUUCCCCUGGUUU 5'
                         ||||||  || || |||||
linc-MD1     :      5' UGGCUGGUCAAACGGAACCAAG 3'       ΔG:-21.13 kcal/mol

mmu-miR-133a :      3' GUCGACCAACUUCCCCUGGUUU 5'
                          |      |     ||||||||
Maml1        :      5' AAAGCAACUACUUUGGACCAAA 3'       ΔG:-13.60 kcal/mol

mmu-miR-133a :      3' GUCGACCAACUUCCCCUGGUUU 5'
                                   |   |||||||
Maml1        :      5' GCUUCCUACCCAGAUGACCAAA 3'       ΔG:-10.81 kcal/mol
-------------------------------------------------------------------------------

mmu-miR-133b :      3' AUCGACCAACUUCCCCUGGUUU 5'
                        | ||||||  || || |||||
linc-MD1     :      5' UGGCUGGUCAAACGGAACCAAG 3'      ΔG:-21.87 kcal/mol

mmu-miR-133b :      3' AUCGACCAACUUCCCCUGGUUU 5'
                          |      |     ||||||||
Maml1        :      5' AAAGCAACUACUUUGGACCAAA 3'      ΔG:-13.70 kcal/mol

mmu-miR-133b :      3' AUCGACCAACUUCCCCUGGUUU 5'
                                   ||  |||||||
Maml1        :      5' GCUUCCUACCCAGAUGACCAAA 3'      ΔG:-10.81 kcal/mol
```

Figure S6

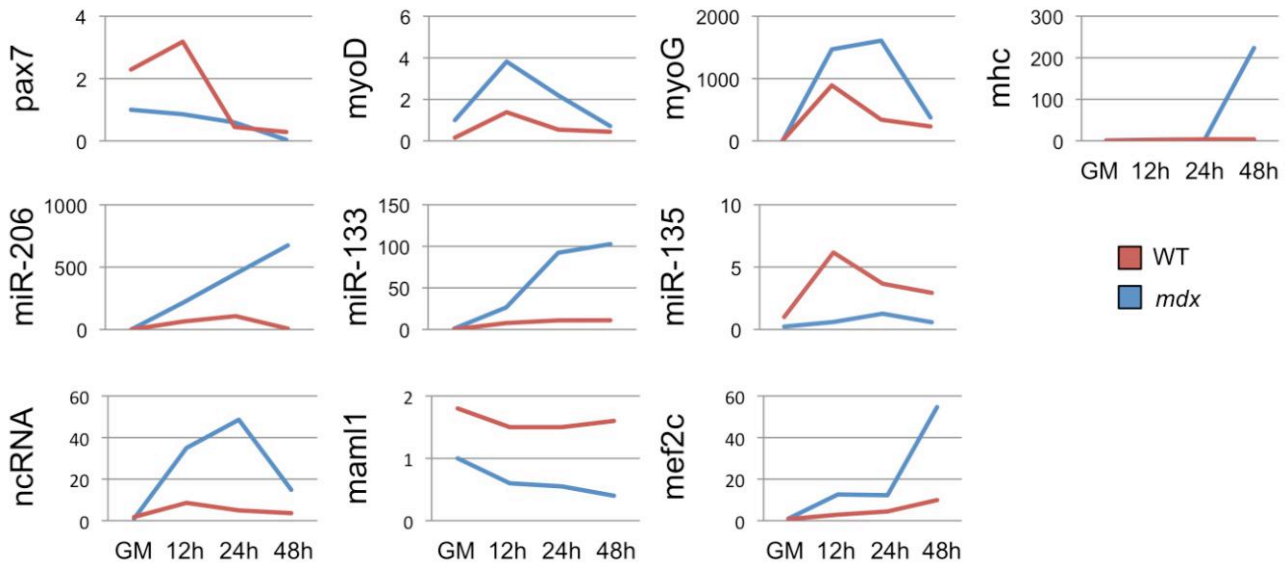
pax7
4
2
0
myoD
6
4
2
0
myoG
2000
1000
0
mhc
300
200
100
0
GM 12h 24h 48h
miR-206
1000
500
0
miR-133
150
100
50
0
miR-135
10
5
0
WT
mdx
ncRNA
60
40
20
0
GM 12h 24h 48h
maml1
2
1
0
GM 12h 24h 48h
mef2c
60
40
20
0
GM 12h 24h 48h

Figure S7

mir	Score	Energy	Note
mmu-miR-683	157	-24.7	(1)
mmu-miR-7a	156	-17.12	(2)
mmu-miR-7b	156	-17.12	(2)
mmu-miR-3058*	153	-27.35	(1)
mmu-miR-135a	151	-16.37	
mmu-miR-135b	150	-16.99	
mmu-miR-370	149	-21.8	(2)
mmu-miR-875-5p	149	-16.75	(1)
mmu-miR-3077*	149	-38.92	(1)
mmu-miR-135b	147	-18.78	
mmu-miR-135a	146	-15.4	
mmu-miR-19b-2*	146	-19.67	(1)
mmu-miR-216b	145	-18.65	(1)
mmu-miR-3084*	145	-13.48	(1)
mmu-miR-450a-2*	145	-18.26	(1)
mmu-miR-133b	144	-21.87	
mmu-miR-133a	144	-21.13	
mmu-miR-320	144	-9.38	(2)
mmu-miR-707	144	-20.44	(1)
mmu-miR-511-5p	143	-21.78	(1)
mmu-miR-703	143	-16.03	(1)
mmu-miR-1968*	143	-17.08	(1)
mmu-miR-3103	142	-9.84	(1)
mmu-miR-340-3p	142	-26.74	(1)
mmu-miR-469	142	-21.41	(1)
mmu-miR-669n	142	-9.11	(1)
mmu-miR-592	142	-9.63	(1)
mmu-miR-1224	142	-20.22	(1)
mmu-miR-653	142	-11.44	(1)
mmu-miR-380-5p	140	-10.7	(1)
mmu-miR-758*	140	-22.04	(1)
mmu-miR-1224*	140	-21.71	(1)
mmu-miR-1905	140	-13.72	(1)
mmu-miR-1-1*	140	-20.49	(1)
mmu-miR-3064-5p	140	-20.85	(1)

Supplementary Table I

Figure S1, related to Figure 1
A) Sequence of the murine linc-MD1 with exons identification, miRNA binding sites and sequence deleted in Δdrosha constructs. B) Conservation pattern of the linc-MD1 transcript expressed as probability of negative selection taken from the Mammal Cons phastCons30wayPlacental track in UCSC database. RF+1, +2 and +3 refer to the reading frames, gray boxes indicate the position of ORFs in number of triplets. The mature transcript contains four open reading frames (defined as any sequence starting with AUG and containing at least 10 non terminator codons) ranging in size from 11 to 91 triplets. None of the AUG shows a Kozak consensus (Kozak 1989), nor are the sequences more or less conserved than the surrounding regions. C) linc-MD1 and miR-206 relative quantifications in the indicated tisses. Values are normalized for HPRT or U6 snRNA respectively and shown with respect to testes sample set to a value of 1.

Figure S2, Related to Figure 1
A) In situ analysis for linc-MD1, in C2 myoblasts in GM and DM. DAPI staining is also shown alone (DAPI) or together with DIG staining (MERGE). Original magnification X20, scale bar 100 μm. B) In situ analysis for linc-MD1, miR-206 in tibialis cryosections from WT and *mdx* animals. DAPI staining is also shown in light blue. Original magnification X20, scale bar 100 μm. In both analyses scramble oligo is used as control.

Figure S3, Related to Figure 2
Northern blot analysis for murine mir-223 expression in C2 myoblasts transfected with D-miR-223 and P-miR-223 constructs and maintained in GM or DM conditions. Ctrl plasmid contains a region between miR-206 and miR-133b, used as negative control. miR-16 was used as loading control.

Figure S4, Related to Figure 4
Schematic representation of pMD-1 and pMD-1-Δdrosha constructs used in linc-MD1 overexpression experiments. Histograms show miR-133 and linc-MD1 RNA relative expression measured by qRT-PCR normalized for U6 snRNA or HPRT respectively and shown with respect to pCtrl set to a value of 1.

Figure S5, Related to Figure 5
A) The constructs described in Figure 5 were co-transfected in C2 myoblasts with scamble LNA (LNA-scr) or LNA for the indicated miRNA. Histograms indicate the values of renilla luciferase measured 48 hours after transfection in DM. Data are shown with respect to the values of RLuc control vector set to a value of 100%. One asterisk: $p<0.05$. B) RLuc/FLuc mRNA ratio measured by qRT-PCR in C2 myoblasts transfected with RLuc-MD1-WT construct together with plasmids expressing miR-133a/b, miR-135a/b or control. Values are normalized for HPRT and shown with respect to pCtrl set to a value of 1.

Figure S6, Related to Figure 5
Base pairing of the miRNAs with their predicted binding sites on linc-MD1 and on their mRNA targets. ΔG values were obtained from miRanda (Enright et al., 2003)

Figure S7, Related to Figure 7
qRT-PCR for the indicated mRNAs and miRNAs in satellite cells purified from WT or *mdx* mice differentiated for the indicated hours. Values are normalized for HPRT or U6 snRNA respectively and shown with respect to GM set to a value of 1.

Supplementary Table I
Summary of miRanda output of conserved miRNAs predicted to bind linc-MD1 sorted according to the miRanda score. Conservation was evaluated using the Mammal Cons phastCons30wayPlacental.

(1) miRNAs not expressed in muscle (see Supplemental Experimental Procedures).
(2) miRNA whose targets are not expressed in muscle or do not have a known function in muscle physiology (see Supplemental Experimental Procedures).

SUPPLEMENTAL EXPERIMENTAL PROCEDURES

Bionformatic analyses

The mature miR sequences were taken from the miRBase database (release 17) (Griffiths-Jones et al., 2008). Linc-MD1 was displayed using the UCSC genome browser (Fujita et al., 2010); genomic locus conservation was evaluated using the Mammal Cons phastCons30wayPlacental (Siepel et al., 2005).
The likelihood of binding of a mature miRNA to linc-MD1 was evaluated using the miRanda package (Enright et al., 2003). After filtering for conservation, 36 putative target sites were identified and are listed in Supplementary Table I.
We identified miRNAs not expressed in muscle (Cacchiarelli et al., 2010; Cardinali et al., 2009) and discarded them. Next, we searched for putative targets of the remaining miRNAs using TargetScan (Friedman et al., 2009). The expression profile of the putative targets in myoblasts (as reported in the GEO database (Barrett et al., 2011) in datasets gds2412 and gds586 (Chen et al., 2006, Tomczak et al., 2004)) were analysed to discard miRNAs whose targets are not expressed in muscle or do not represent valuable targets in muscle physiology according to Ashburner et al. (2000) (see Supplementary Table I).
Transcription factor binding sites were predicted using RVista Algorithm (Loots et al., 2004).

RNA and protein analyses

Total RNA was prepared from liquid nitrogen-powdered tissues or cell cultures using miRNeasy (QIAGEN). miRNA and mRNA analyses were performed using miScript System (QIAGEN). Relative quantification was performed using, as endogenous controls, U6 snRNA for miRNAs and HPRT1 for mRNAs. PolyA+ RNA fraction was obtained using oligodT affinity purification (QIAGEN). Northern blot for miRNAs was performed according to Cacchiarelli et al. (2010) while Northern blot for linc-MD1 was performed on purified polyA+ RNA, using a radioactive probe obtained by nick-translation. RNA in situ hybridization was performed in formaldehyde and carbodiimide (EDC)-fixed gastrocnemius cryosections or cell cultures, according to Cacchiarelli et al. (2010). Primers sequences for ncRNA detection are listed in supplementary experimental procedures ; Western blot on total extracts were performed as described in Denti et al. (2006).

RACE analyses

5' RACE analyses were performed choosing reverse primers surrounding pre-miRNA sequences while 3'RACE forward primers were designed to validate putative polyadenylation sites indicated in Figure 1B. cDNA synthesis, PCR and nested-PCR were performed according to manufacturer's specifications (Invitrogen).

Reporter constructs and luciferase assays

Distal (DIST) and proximal (PROX) elements were tested using two types of reporter constructs. DIST and PROX were cloned in a Pgl3basic (Promega) modified plasmid in which firefly luciferase gene was substituted with murine pre-miR-223 sequence. The same regions were also cloned in a Pgl4.10 FLuc reporter plasmid (Promega) individually (D-FLuc or P-FLuc) or in combination as enhancer assay (D-FLuc-P or P-FLuc-D). Transfection efficiency of these constructs were assessed by co-transfection of pRLTK plasmid (Promega) encoding for renilla luciferase gene.
Exon 1, exon 2 and exon 3 sequence of linc-MD1 cDNA (RLuc-MD1-WT) were amplified by PCR and cloned in Ψcheck2 plasmid (Promega), downstream renilla luciferase gene

(RLuc). The same plasmid also contains the firefly luciferase gene (FLuc) to normalize for transfection efficiency. Mutant derivatives (RLuc-MD1-Δ133 and RLuc-MD1-Δ135) were obtained by deletion of miR-133 and miR-135 binding sites indicated in Figure S1 by inverse PCR. The same procedure was followed for the production of maml1 and mef2c 3'UTR reporter constructs (RLuc-maml1-WT and RLuc-mef2c-WT) and their mutant derivatives (RLuc-maml1-*mut* and RLuc-mef2c-*mut*).
RLuc and FLuc activities were measured by Dual Glo Luciferase assay (Promega).

Overexpression constructs

Constructs for the over-expression of linc-MD1 were obtained by cloning linc-MD1 cDNA (Figure S1) in pCDNA3.1- plasmid (Invitrogen) and all mutants were obtained by inverse PCR. Lentiviral constructs were obtained by subcloning the CMV-lincMD1-BGH cassette into HpaI site of PCCL-gfp plasmid (Incitti et al., 2010).
miRNA overexpression constructs were obtained by cloning 100 nucleotides upstream and downstream from the pre-miRNA of interest into the U1snRNA expression cassette (Cacchiarelli et al., 2010).

Statistical analyses

The data shown in the histograms are the result of at least three independent experiments performed on at least three samples or animals. Unless stated otherwise, data are shown as mean ± standard deviation and statistical significance of differences between means was assessed by two-tailed t-test and $P<0.05$ was considered significant.

Oligonucleotides

murine linc-MD1 detection by RT-PCR
mmu_LINC_MD1_FW - tggagtgattgaggtggaca
mmu_LINC_MD1_RV – tgatggcaaaaccagcatta

murine and human linc-MD1 detection by qRT-PCR
mmu_LINC_MD1_FW - gcaagaaaaccacagaggagg
mmu_LINC_MD1_RV - gtgaagtccttggagtttgag
hsa_LINC_MD1_FW - cactgccagctctggaaaat
hsa_LINC_MD1_RV – acttggttccgtttgaccag

murine linc-MD1 cloning in ψcheck2 and pCDNA3.1-
mmu_LINC_MD1_cdna_FW - ctctttgcagtgggacagct
mmu_LINC_MD1_cdna_RV – tgatggcaaaaccagcatta

5' RACE reverse oligos for RT and subsequent nested PCR
MIR206_RT - atgtagccaaggaacgaaga
MIR206_PCR_OUTER - tcacgcagaaaggaaaagc
MIR206_PCR_INNER - acttcatccattctacactccc
MIR133B_RT - cttcttgggaacataaggcta
MIR133B_PCR_OUTER - tgaagtccttggagtttgagc
MIR133B_PCR_INNER – ggagtttgagcaccacttgtc

3' RACE forward oligos for nested PCR
3'RACE_outer - catctaaattacaagaaaacaaga
3'RACE_inner - ctataactgtattccattttcgtg

PROMOTER CLONING
Prox_FW - ggacccttcttctcctctta
Prox_RV - caggcgctattgtacttc

Dist_FW - atggctaccttgtcagcacttcc
Dist_RV - gcctcttccctttgtactttcc

Oligonucleotide sequences for Chip, 3C as well as plasmids and other material are available upon request.

References

- Ashburner, M., et al. (2000) Gene ontology: tool for the unification of biology. The Gene Ontology Consortium. Nat Genet. *25*, 25-29.
- Barrett, T., et al. (2011) NCBI GEO: archive for functional genomics data sets—10 years on. Nucleic Acids Res. 39(Database issue):D1005-10
- Cardinali, B, et al. (2009). Microrna-221 and microrna-222 modulate differentiation and maturation of skeletal muscle cells. PLoS One. *4*, e7607.
- Denti, M.A. et al. (2006). Body-wide gene therapy of Duchenne Muscular Dystrophy in the mdx mouse model. Proc. Natl. Acad. Sci. *103*, 3758-3763.
- Friedman, R.C., Farh, K.K., Burge, C.B., and Bartel, D.P. (2009). Most Mammalian mRNAs Are Conserved Targets of MicroRNAs Genome Res., *19*, 92-105
- Fujita, P.A. et al. (2010). The UCSC Genome Browser database: update 2011. Nucleic Acids Res., *39,* D876-82.
- Griffiths-Jones, S., Saini, H.K., van Dongen, S. and Enright, A.J. (2008). miRBase: tools for microRNA genomics. Nucleic Acids Res., *36*, D154-D158.
- Kozak, M. (1989). The scanning model for translation: an update. J. Cell Biol, *108*, 229-241.
- Loots G. and Ovcharenko I. (2004). rVista 2.0: evolutionary analysis of transcription factor binding sites. Nucleic Acids Research, *32*, W217-W221
- Siepel, A. et al., (2005). Evolutionarily conserved elements in vertebrate, insect, worm, and yeast genomes. Genome Res., *15*, 1034-1050.
- Tomczak KK, Marinescu VD, Ramoni MF, Sanoudou D, Montanaro F, Han M, Kunkel LM, Kohane IS, Beggs AH. (2004). Expression profiling and identification of novel genes involved in myogenic differentiation. FASEB J., *18*, 403-405.

Supplemental Figure 1
Click here to download high resolution image

SUPPLEMENTAL FIGURES & TABLES

A

mmu-linc-MD1 (conserved exonic sequences)

```
  1  CTCTTTGCAGTGGGACAGCTGAAGAGGTATAATTTAACAGCTTTCAGAAG  50
 51  CCCGTCACTGGAGTGATTGAGGTGGACAGAAGGCAGGGACATGACCACGG 100
101  TCCTTAAAAGACACAAACAGGATTCTGACAGGAAGCCATAGAAATGCAAG 150
151  CCAACACTGCCAGCTCTGGAAATAAATAAATAATGACCCAGGTTCTATGC 200
201  TCCTCAATGGGGGCAGAAGCCTGCGGGGCAAGAAAACCACAGAGGAGGAG 250
251  GGACCTGCCTGCAACTTGTCCCCAGGCTTGGACAAGTGGTGCTCAAACTC 300
301  CAAGGACTTCACAAGCTTCAGGCTGCAGTCACCTCCAAAGGGAGTGGCCC 350
351  CCTGCTCTGGCTGGTCAAACGGAACCAAGTCCGTCTTCCTGAGAGGTTTG 400
401  GTCCCCTTCAACCAGCTACAGCAGGGCTGGCAAAGCTCAATATTTGGAGA 450
451  AAGAGAAGAGAAGAGAAAATAGCTGCTACAGCCTTGCTTATGAAAAGTAA 500
501  TGCTGGTTTTGCCATCATAGC..... 550
```

EXON1 – EXON2 – EXON3 – pre-miR-133b
AAGCCA – miR-135 seed
AACCAA – miR-133 seed
CCCCTTCAACCAGCTACAGCAGGG - Δdrosha deletion

B

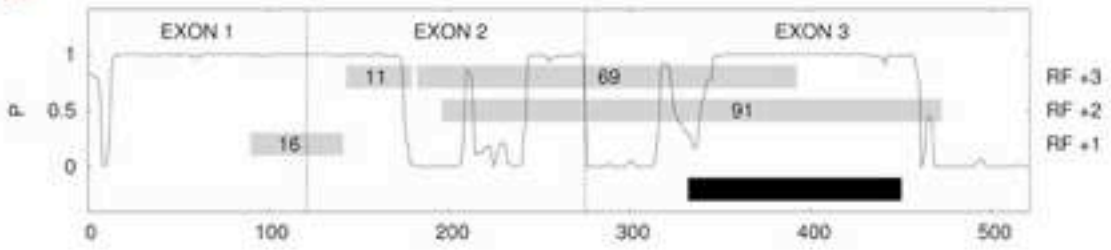

C

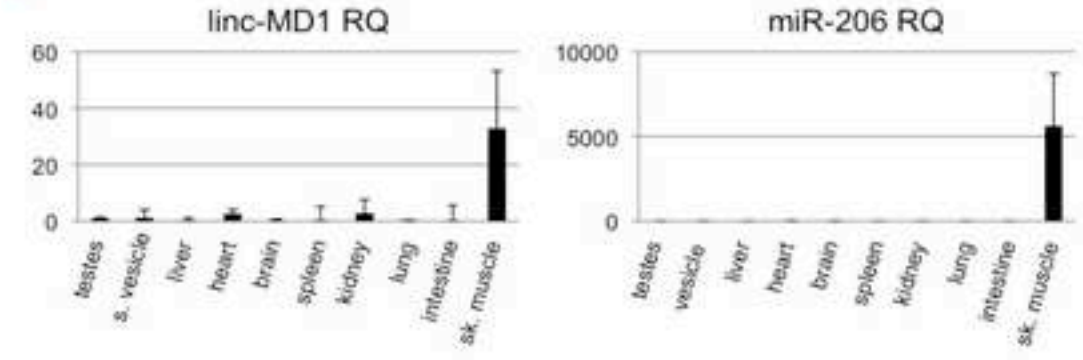

Figure S1

Supplemental Figure 2

Click here to download high resolution image

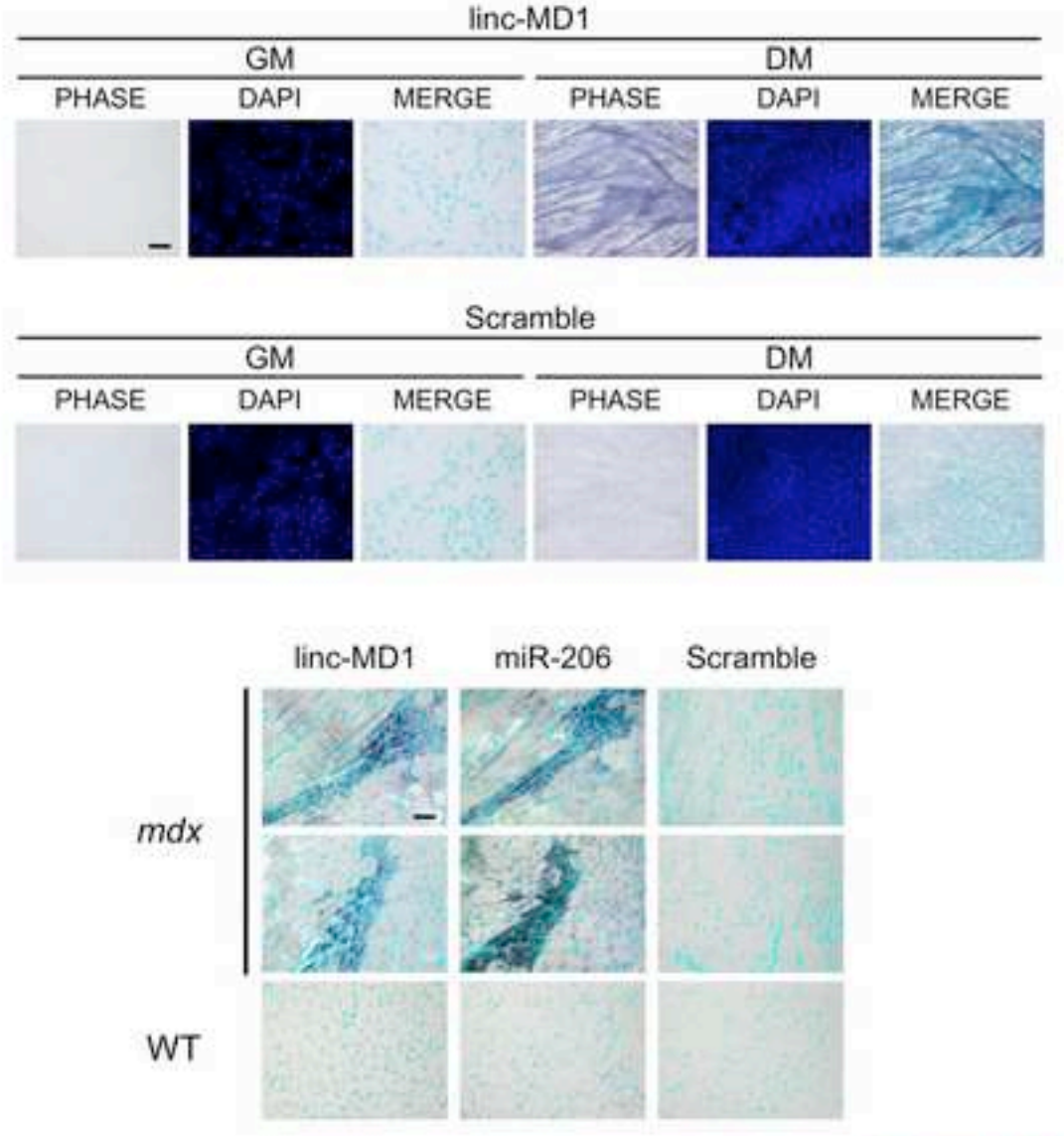

Figure S2

Supplemental Figure 3

Click here to download high resolution image

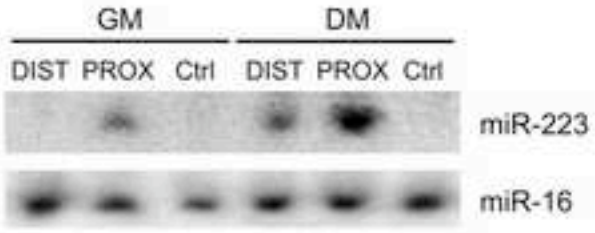

Figure S3

Supplemental Figure 4

Click here to download high resolution image

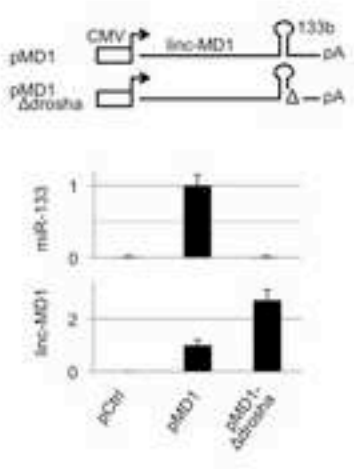

Figure S4

Supplemental Figure 5

Click here to download high resolution image

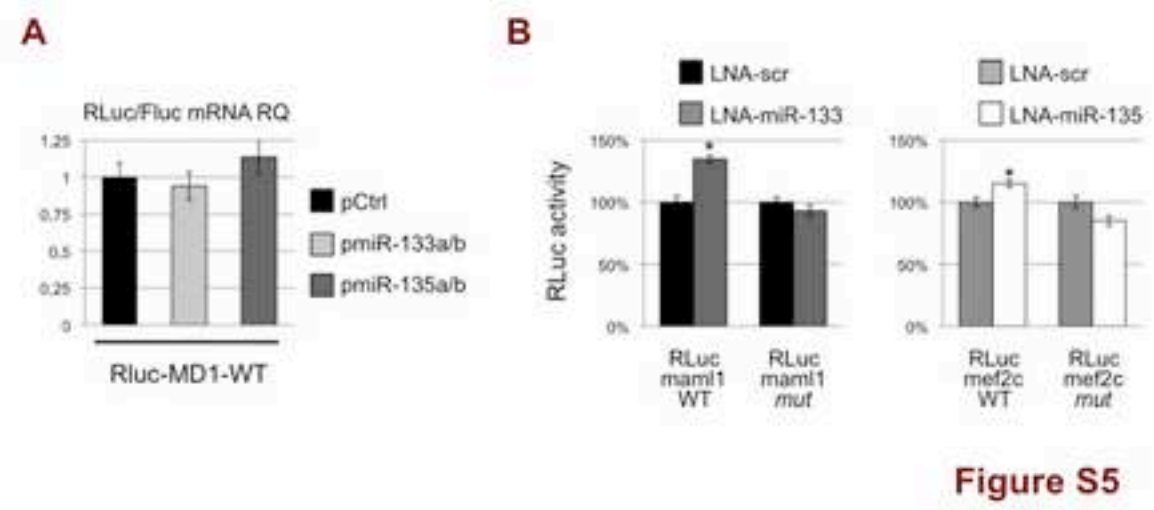

Figure S5

Supplemental Figure 6

Click here to download high resolution image

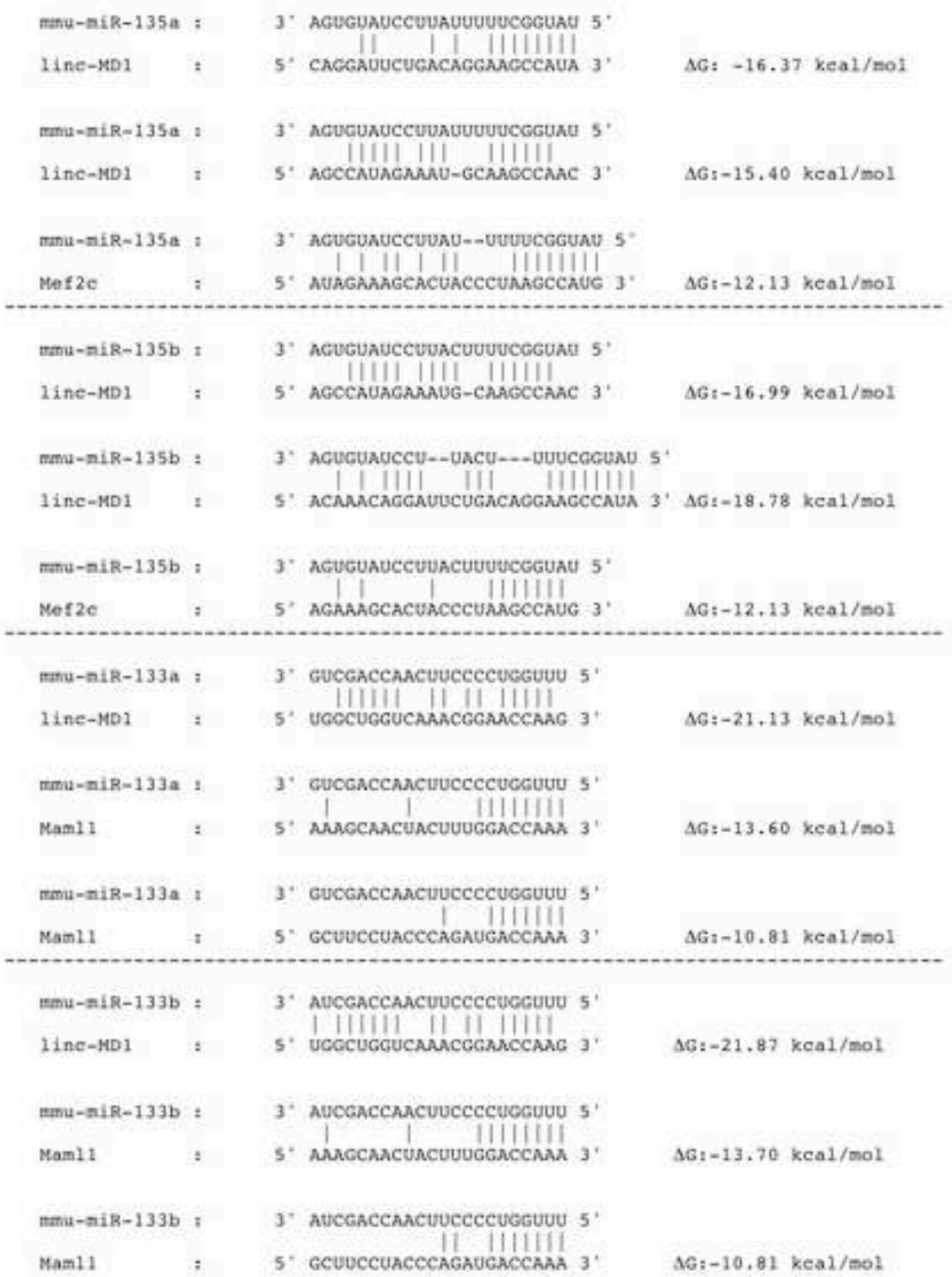

Figure S6

Supplemental Figure 7

Click here to download high resolution image

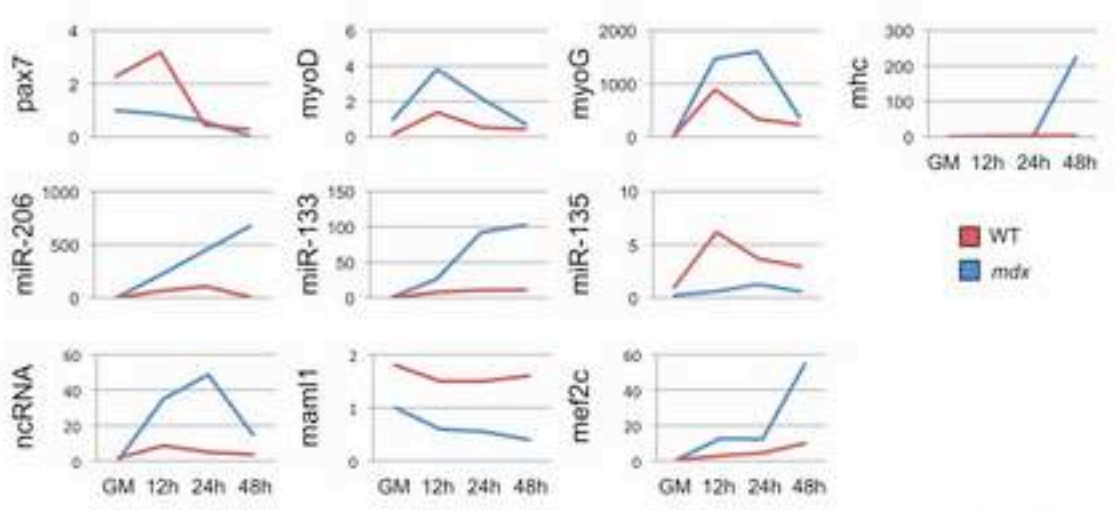

Figure S7